January 7, 2022

Deborah Trent
[redacted]

Linda Jackson, Payette Forest Supervisor
Stibnite Gold Project
500N. Mission St., Building 2
McCall, ID. 83638

Ms Jackson,

I am commenting about what appears to be a major shift in direction from the mining of gold, to the mining of Antimony. The recent large sum of money from the US Department of Defense to Perpetua Resources to do an environmental and engineering studies on antimony trisulfide, has me very concerned.

There has been recent research about Antimony in 2021 by a group of International Scientists (see enclosed document: Environment International) that proves that the mining of Antimony is potentially toxic to ecosystems and public health via the accumulation in the food chain. However, there are gaps in understanding how poisonous and carcinogenic it is. Also unclear is what are the mechanisms that cause the toxicity.

Antimony in certain biochemical states is one of the most explosive elements on earth! The transportation, storing, and processing of it is very dangerous. Will it be stored on site? If not where and what kind of transport in and out of the mountains and on our Highways 55 and 95 would permit it? What if there was a fire in the area that would come into contact with it? OR God forbid, an act of terrorism?

If Antimony leaches into the South Fork of the Salmon or Antimony dust particles build up in the soils, how would this affect fish, wildlife, and the entire ecosystem for years to come?

It seems to me that there is no amount of money in the world that would cover all these "what ifs" with a 100% guarantee that some sort of event could be avoided. Any of these situations could happen and the close proximity to our communities and Wild and Scenic Salmon River, would be complete devastation.

The RISKS OUTWEIGH THE BENEFITS here. This is a short term bad decision that could have very irreversible long term damaging consequences.

Please, chose the NO- Action alternative! I do not see any way that the Stibnite Mine should be allowed to proceed.

Sincerely,

Deborah Trent

Environment International 158 (2022) 106908

Contents lists available at ScienceDirect

Environment International

journal homepage: www.elsevier.com/locate/envint

Antimony contamination and its risk management in complex environmental settings: A review

Nanthi Bolan[a,b,c,*], Manish Kumar[d], Ekta Singh[d], Aman Kumar[d], Lal Singh[d], Sunil Kumar[d], S. Keerthanan[e], Son A. Hoang[c], Ali El-Naggar[f], Meththika Vithanage[e], Binoy Sarkar[g], Hasintha Wijesekara[h], Saranga Diyabalanage[e], Prasanthi Sooriyakumar[e], Ajayan Vinu[c], Hailong Wang[i,j], M.B. Kirkham[k], Sabry M. Shaheen[l,m,n], Jörg Rinklebe[l,o,*], Kadambot H. M. Siddique[a,b]

[a] *School of Agriculture and Environment, The University of Western Australia, Perth, WA 6001, Australia*
[b] *The UWA Institute of Agriculture, The University of Western Australia, Perth, WA 6001, Australia*
[c] *Global Innovative Centre for Advanced Nanomaterials (GICAN), College of Engineering, Science and Environment, The University of Newcastle Callaghan, NSW 2308, Australia*
[d] *CSIR-National Environmental Engineering Research Institute (CSIR-NEERI), Nehru Marg, Nagpur 440020, Maharashtra, India*
[e] *Ecosphere Resilience Research Center, Faculty of Applied Sciences, University of Sri Jayewardenepura, Nugegoda 10250, Sri Lanka*
[f] *Department of Soil Sciences, Faculty of Agriculture, Ain Shams University, Cairo 11241, Egypt*
[g] *Lancaster Environment Centre, Lancaster University, Lancaster LA1 4YQ, UK*
[h] *Department of Natural Resources, Faculty of Applied Sciences, Sabaragamuwa University, Belihuloya 70140, Sri Lanka*
[i] *Biochar Engineering Technology Research Center of Guangdong Province, School of Environmental and Chemical Engineering, Foshan University, Foshan, Guangdong 528000, People's Republic of China*
[j] *Key Laboratory of Soil Contamination Bioremediation of Zhejiang Province, School of Environmental and Resource Sciences, Zhejiang A&F University, Hangzhou, Zhejiang 311300, People's Republic of China*
[k] *Department of Agronomy, Kansas State University, Manhattan, KS, United States*
[l] *University of Wuppertal, School of Architecture and Civil Engineering, Institute of Foundation Engineering, Water- and Waste Management, Laboratory of Soil- and Groundwater-Management, Pauluskirchstraße 7, 42285, Germany*
[m] *King Abdulaziz University, Faculty of Meteorology, Environment, and Arid Land Agriculture, Department of Arid Land Agriculture, Jeddah 21589, Saudi Arabia*
[n] *University of Kafrelsheikh, Faculty of Agriculture, Department of Soil and Water Sciences, 33 516 Kafr El-Sheikh, Egypt*
[o] *Department of Environment, Energy and Geoinformatics, Sejong University, 98 Gunja-Dong, Seoul, Republic of Korea*

ARTICLE INFO

Handling editor: Hefa Cheng

Keywords:
Toxic metal(loid)s
Soil environments
Aquatic environments
Biogeochemical processes
Risks and remediation approaches

ABSTRACT

Antimony (Sb) is introduced into soils, sediments, and aquatic environments from various sources such as weathering of sulfide ores, leaching of mining wastes, and anthropogenic activities. High Sb concentrations are toxic to ecosystems and potentially to public health via the accumulation in food chain. Although Sb is poisonous and carcinogenic to humans, the exact mechanisms causing toxicity still remain unclear. Most studies concerning the remediation of soils and aquatic environments contaminated with Sb have evaluated various amendments that reduce Sb bioavailability and toxicity. However, there is no comprehensive review on the biogeochemistry and transformation of Sb related to its remediation. Therefore, the present review summarizes: (1) the sources of Sb and its geochemical distribution and speciation in soils and aquatic environments, (2) the biogeochemical processes that govern Sb mobilization, bioavailability, toxicity in soils and aquatic environments, and possible threats to human and ecosystem health, and (3) the approaches used to remediate Sb-contaminated soils and water and mitigate potential environmental and health risks. Knowledge gaps and future research needs also are discussed. The review presents up-to-date knowledge about the fate of Sb in soils and aquatic environments and contributes to an important insight into the environmental hazards of Sb. The findings from the review should help to develop innovative and appropriate technologies for controlling Sb bioavailability and toxicity and

---

* Corresponding authors at: School of Agriculture and Environment, The University of Western Australia, Nedlands, Western Australia, Australia (N. Bolan). University of Wuppertal, School of Architecture and Civil Engineering, Institute of Foundation Engineering, Water- and Waste Management, Laboratory of Soil- and Groundwater-Management Pauluskirchstraße 7, 42285 Wuppertal, Germany (J. Rinklebe).

E-mail addresses: nanthi.bolan@uwa.edu (N. Bolan), rinklebe@uni-wuppertal.de (J. Rinklebe).

Recent Research

https://doi.org/10.1016/j.envint.2021.106908
Received 19 July 2021; Received in revised form 3 September 2021; Accepted 27 September 2021
Available online 4 October 2021

sustainably managing Sb-polluted soils and water, subsequently minimizing its environmental and human health risks.

1. Introduction

Antimony (Sb) is one of the most commonly used metallic element, with global reserve of 1.9 million tons. According to recent report, almost 80% of Sb production was concentrated in China, Russia, and Bolivia (United States Geological Survey, 2021). By 2020, China was the leading producer of Sb worldwide, accounting for nearly 80,000 metric tons, and Russia the second highest (Statista, 2021). Sb is most commonly used as a fire retardant in various products such as toys, car-seat covers, light-aircraft-engine covers, and clothing for children and fire fighters (Bagherifam et al., 2019a, Filella et al., 2020, Hu et al., 2021), which accounts for around 60% of global Sb consumption. Sb is also frequently used as a glass decolorizer, a catalyst in plastic production, in the manufacture of paint pigments, and in metal alloys for ammunition and battery production (Diquattro et al., 2021; Guo et al., 2018; Okkenhaug et al., 2016). Sb is released into soils and aquatic environments from several sources, the weathering of sulfide ores, leaching from mining wastes, and anthropogenic activities such as smelting, metallurgical operations, and shooting (Diquattro et al., 2020; Diquattro et al., 2021). For example, in the vicinity of the world's biggest Sb-mining site in Hunan Province, China, Sb concentrations in mining soils range from 101 to 5,045 mg kg^{-1} (He, 2007), and from 17 to 288 µg L^{-1} in water samples (Guo et al., 2018; Wang et al., 2011). In the Extremadura province of Spain, Sb concentrations at three abandoned Sb-mining areas range from 225 to 2,449 mg kg^{-1} (Murciego et al., 2007). In the United States (U.S), an estimated 1,900 tons of Sb have been released from approximately 3,000 military shooting ranges and 9,000 public shooting ranges (Wan et al., 2013). Shooting-range soils are considered a key anthropogenic source of Sb in several countries (Okkenhaug et al., 2013), notably Australia (Sanderson et al., 2014), Korea (Ahmad et al., 2014), Finland (Sorvari, 2007), Norway (Strømseng et al., 2009), and Canada (Laporte-Saumure et al., 2011).

Similar to arsenic (As), Sb possesses an s^2p^3 outer orbital electron configuration and thus occurs in the form of (–III, 0, +III, and + V) (Diquattro et al., 2020). In the natural pH range (3–10), the deprotonated state of antimonic acid or $Sb(OH)_6^-$ is the predominant Sb(V) species, which is stable over a wide range of soil reduction–oxidation (redox) potential, whereas under anaerobic conditions, Sb(III) occurs as neutral antimonous acid ($Sb(OH)_3$) (Diquattro et al., 2020; Rinklebe et al., 2020). $Sb(OH)_6^-$ has also been found the leading form in polluted sites close to mineral ore smelteries and at shooting ranges (Johnson et al., 2005; Takaoka et al., 2005).

A high Sb concentration in soil or sediments is toxic to ecosystems, and potentially affects human health via accumulation in the food chain (Antoniadis et al., 2019; Shaheen et al., 2019, Shahid et al., 2019). Once entering human bodies by either direct (inhalation or ingestion) or indirect (via the food chain) exposure, Sb and Sb-derived compounds react with sulfhydryls in human tissue, leading to cellular hypoxia by inhibiting enzymatic action and disturbing cellular ionic balance. These adverse impacts eventually result in metabolic malfunctioning and impairment of the nervous system and as vital organs (Yang et al., 2015). Generally, the toxicity of various Sb speciation is in the following order: antimonite (III) > antimonite (V) > organo-antimonials (e.g., methylated species) (Wei et al., 2015). Sb is classed as a priority contaminant by both the US Environmental Protection Agency (USEPA) and the Council of the European Union (EU) (Bagherifam et al., 2019b; Hua et al., 2021). The maximum acceptable values of Sb in consumable water and soil regulated by the World Health Organization (WHO) are 0.020 mg L^{-1} and 36 mg kg^{-1}, respectively (Chang et al., 2002; Guo et al., 2009).

Human toxicity of Sb(III), a reduced form of Sb, is tenfold higher than that of the oxidized form (Sb(V)) (Filella et al., 2020). Xue et al. (2017) reported entry of Sb into the human body via ingestion of a contaminated diet and dermal contact, which eventually disturbs the viability, formation, and secretion of metallothionein proteins. Excessive ingestion of Sb by humans can lead to nausea, diarrhea, skin rashes, and respiratory disorders (Hua et al., 2021). The International Agency for Research on Cancer (IARC) reported that Sb trioxide (Sb_2O_3) is a possibly oncogenic substance to humans (IARC, 1989). Further studies by the IARC with Sb_2O_3 revealed unconvincing or unclear results. More recently, the US National Toxicology Program (US-NTP) said that Sb_2O_3 is a human carcinogen based on carcinogenicity tests on model organisms and results from mechanistic investigations (NTP, 2018). Still, the available data related to Sb carcinogenicity on humans are insufficient to evaluate the relationship between people exposed to Sb_2O_3 and human cancer risk.

Remediation of Sb in soil and water ecosystems can be achieved through immobilization, mobilization of Sb using various amendments, and removal through phytoremediation and bioremediation (Diquattro et al., 2021; Hua et al., 2021; Loni et al., 2020; Sun et al., 2017; Zand and Heir, 2020) (Fig. 1). A range of materials has been explored to mitigate Sb risk based on adsorption and immobilization, including activated carbon (Yu et al., 2014), biocomposite materials (Lapo et al., 2019), biochar (Jia et al., 2020), metal oxides (Wang et al., 2019a), mineral sorbents (Zhang et al., 2020), imprinted polymers (Shakerian et al., 2014), and nano zero-valent iron (Huang et al., 2019). Recent literature mentioned the effects of different soil amendments in remediation of Sb-impacted sites in terms of reducing bioavailability and toxicity of the contaminant (Li et al., 2018b; Palansooriya et al., 2020; Rinklebe et al., 2020). Filella and Williams, (2012) and Filella, (2011) previously reviewed, how Sb interact with heterogeneous complexants of the environments which influence their speciation, bioavailability, and further remediation. Furthermore, few recent reviewed discussed the distribution of Sb in various environmental compartments, along with their remediation technologies (Long et al., 2020b; Li et al., 2018b; Artzer et al., 2018). More recently, Nishad and Bhaskarapillai, (2021) reviewed the industrial release of Sb in the environments and their remediation via various physicochemical and biological approaches. However, there

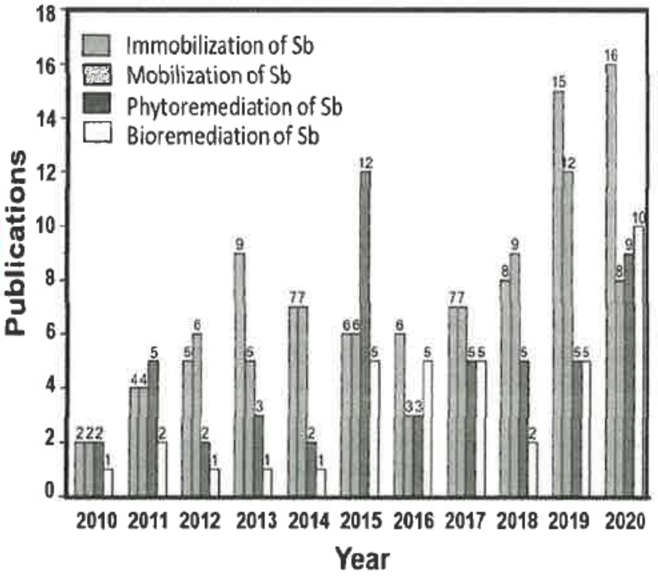

Fig. 1. Number of publications (2010–2020) related to remediation of antimony via various processes.

is no comprehensive review on the biogeochemistry and transformation of Sb related to Sb remediation.

Therefore, the present review integrates the fundamental aspects of Sb transformation and recent developments in understanding Sb speciation and bioavailability related to the remediation of Sb-contaminated terrestrial and aquatic ecosystems. This review presents the current knowledge on the fate of Sb in soils and aquatic environments, contributing to a better cognizance of the environmental hazards of Sb.

2. Origin and sources of Sb contamination

Sb enters the environment via naturally occurring geogenic and anthropogenic pathways. Consequently, it appears in diverse environmental components, including surface and groundwater, soil, sediment, rock, and air (Fig. 2).

2.1. Geogenic sources

Sb is found throughout various environmental compartments (e.g., soil, water, air), and in most biota (Fort et al., 2016; Hiller et al., 2012). Compared to other elements occurring in the earth's crust, the abundance of Sb is low, ranging from 0.2 to 0.3 μg g^{-1}. The abundance of Sb in rocks is usually between 0.2 μg g^{-1} and several μg g^{-1}, but its higher abundance in shale can reach up to 300 μg g^{-1} (Zhuang et al., 2018). Sb is present in organic or inorganic form(s) (Qi et al., 2008; Zhuang et al., 2018), predominant in pyrites and several other sulfide minerals (Vikent'eva and Vikentev, 2016). Sb is a scarce element and, in the usual environmental setting, often exists in the forms of stibnite (Sb_2S_3) and Sb bloom (Sb_2O_3) (Zhuang et al., 2018).

Sb concentrations fluctuate under various environmental, geological, and biogeochemical conditions, due to leaching and its continuous release from ores, minerals, and associated rocks (Ahmad et al., 2014; Okkenhaug et al., 2016). Sb exists in clay-mineral deposits and is associated with the organic matter of coal (Qi et al., 2008). For instance, anomalous Sb in coals is associated with the characteristics of its source areas, including low-temperature magmatic-hydrothermal liquids, volcanic remnants, and groundwater (Qi et al., 2008). Sb in coals is positively correlated with its sulfide form (Qi et al., 2008). Occasionally, pentavalent antimony (Sb(V)) and the more lethal trivalent antimony (Sb(III)) are detected in natural water environments (NHMRC and NRMMC, 2011). Moreover, Sb can be recovered by converting Sb(III) sulfide to its oxide and reducing it with carbon (Coughlin et al., 2020).

Sb is found naturally in sedimentary rocks, soils, and water at 0.15–2 mg kg^{-1}, 0.3–8.6 mg kg^{-1}, and < 1 μg mL^{-1}, respectively (Pierart et al., 2015). As with most minerals, Sb concentrations are dependent on parent materials, with a typical range of 0.2–10 mg kg^{-1}, but usually under 1 mg kg^{-1} (Tschan et al., 2009). Sb levels in clean water and sea water are < 1 μg L^{-1} and 0.2 μg L^{-1}, respectively, and up to 100 μg L^{-1} in the vicinities of an anthropogenically contaminated water (Filella et al., 2002). Guideline values for acceptable Sb levels in potable water are set at 20 μg L^{-1} (WHO, 2011) and 5.0 μg L^{-1} (Council of the European Union, 1998). The Australian Drinking Water Guidelines note that concentrations of Sb in potable water should not exceed 3 μg L^{-1} (NHMRC and NRMMC, 2011).

2.2. Anthropogenic sources

The primary source of the hazardous form of Sb (i.e., Sb(V)) mainly originates from industrial activities, such as metal mining and pharmaceutical manufacturing (Zhuang et al., 2018). Other sources include

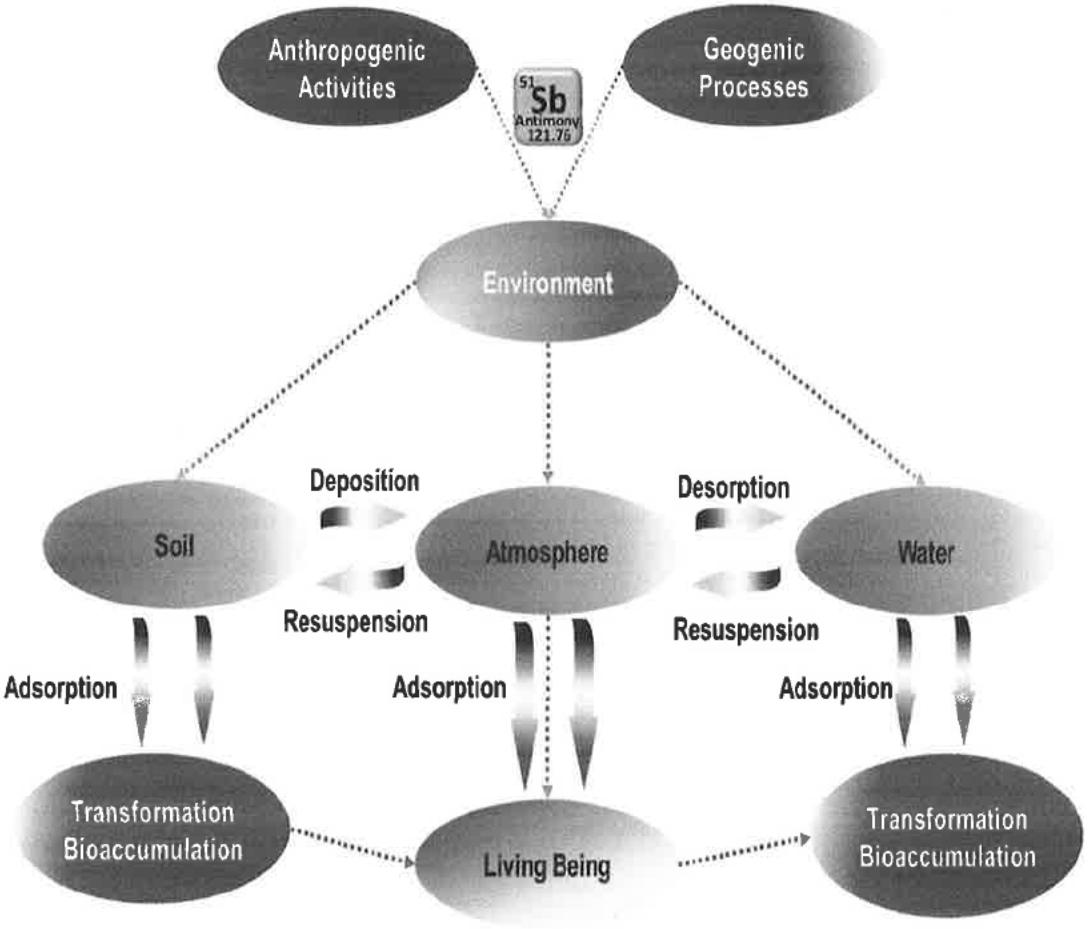

Fig. 2. Antimony sources, transformation, and principal pollution pathways.

sewage sludge (Campos et al., 2019), vehicular emission (Fort et al., 2016), leaching from plastic waste (Chu et al., 2021; Hu et al., 2021), seepage from mining wastes and industrial dumps (Dupont et al., 2016), direct infiltration of leachate from landfill disposal of solid wastes or electronic wastes (Intrakamhaeng et al., 2020), and spillage from industrial metal processing or wood preserving facilities (Herath et al., 2017). Antimonial compounds were first used in ancient times. Sb was found in a 5,000-year-old vase now in the Louvre Museum in Paris (France) and yellow-lead-antimonite-glazed ornamental bricks at Babylon that date from 604 to 561 BCE. Roman Sb-decolourized glass fragments in the Yasmina Necropolis at Carthage provide archaeological evidence of Sb usage prior to the mid-fourth century BC (Schibille et al., 2017). Rom-Sb glasses were recycled and then mixed to produce Rom-Sb-Mn by Romans (Schibille et al., 2017). In modern times, Sb alloys and compounds are also necessary in many manufacturing industries (e.g., semiconductors, motor vehicle batteries, flameproofing materials, pesticides, solder alloys, and fireworks), and in the process of car-tire vulcanization (Bagherifam et al., 2019a; Diquattro et al., 2021; Guo et al., 2018; NHMRC and NRMMC, 2011; Okkenhaug et al., 2016).

Lead bullets used in small-arm shooting ranges are hardened by the addition of 2–8% Sb (Mariussen et al., 2017). As a result, small arm shooting ranges are polluted by the accretion of heavy metal(loid)s into soils, where the key pollutants are lead (Pb), copper (Cu), and Sb. Mariussen et al. (2017) reported that nearly 12 tons of Sb are deposited annually at the Steinsjøen military shooting range in Østre Toten in southern Norway. Sb is mainly present as uncharged Sb(III) ($Sb(OH)_3$) and anionic Sb(V) ($Sb(OH)_6^-$) in soil pore water, which is an easily dissolved oxyanion that depends on soil redox conditions and pH. Mariussen et al. (2017) used iron grit and ferric oxyhydroxide powder, along with limestone, as sorption amendments added to the soil to restrict cation exchange in pore water, which is responsible for Sb(V) mobility. In that study, Sb(V) species dominated in both treated and untreated soil pore-water measurements and the Sb(III) level was less than the limit of detection (0.21 μg L^{-1}).

The rising environmental plastic and plastic fragments and their management are of global concern (Sridharan et al., 2021a, b; Kumar et al., 2020a; Kumar et al., 2020b). Sb is used as a co-active fire retardant or an additive or catalyst in plastics products (Chu et al., 2021; Turner, 2018; Turner and Filella, 2017). For instance, Turner and Filella (2017) showed that Sb was present in 18% of >800 polymeric, consumable, and daily-use products, including plastics and plastic fragments, rubber, fabrics, fibers, and foams. In 2020, the worldwide production of Sb was assessed to be around 153,000 tons and almost 14% (22,000 tons) of the worldwide production was consumed by the U.S. (United States Geological Survey, 2021). Due to its utilization as an additive in products and its inadequate recycling, the quantity of Sb discharged into natural settings slowly increases (Hu et al., 2021), which poses a threat to health, mainly from the extremely toxic Sb(III) and its associated compounds (He et al., 2019a). Chu et al., (2021) investigated the anthropogenic release of Sb into the environment from polyethylene terephthalate (PET) during different stages of fabrication using a network-model analysis. They reported that the manufacturing of PET released 2,926 tons, followed by its dyeing (2,223 tons) and weaving (908 tons). Disposal of waste PET fibers released 1,108 tons of Sb in landfills. Discarded fiber waste not put in landfills was 872 tons. Mechanical recycling, chemical recycling, and incineration processes released respectively 784, 284, and 25 tons of Sb into the environment (Chu et al., 2021).

Historic Sb mine sites with unmanaged wastes are a serious environmental hazard because they regularly release Sb into the surrounding environment (Dupont et al., 2016; Fu et al., 2016; Hu et al., 2021; Intrakamhaeng et al., 2020) (Table 1). Soils surrounding unrestrained Sb mines are often severely polluted with As and Sb (Wilson et al., 2010). Moreover, precipitation can enable mobilization of soil Sb into surface waters and groundwater (Hiller et al., 2012), which diminishes the quality of the waters and introduces pollutants into the food chain

Table 1
Selected references on different sources and levels of Sb in soil and water.

Country	Media	Source of contamination	Concentration level (Soil-mg kg^{-1}) and (Water-mg L^{-1})	Reference
Australia	Soil	Floodplain back-swamp	16.6 ± 1.5	Wilson et al. (2014)
		Floodplain levee	8.3 ± 0.5	
		Control	0.2 ± 0.1	
		Rhizosphere soil	9.6–23.5	
Britain	Soil	Former mining and smelting sites	11.94–709.8	Flynn et al. (2003)
China	Soil	Mining	528 ± 259	He et al. (2012)
		Tailing Dam	564 ± 252	
	Soil	Forestry	115 ± 72	
	Soil (roadside	Vegetation	49.75 ± 34.80	
	Soils near	Grassland	39.29 ± 28.36	
	industry)	Coals	2.27	Qi et al. (2008)
		Baosteel Co., Ltd.	3.39 ± 3.59	Yan et al. (2020)
		Gaoqiao Petrochemical Co., Ltd.	2.88 ± 1.39	
		Jiangqiao Domestic Garbage Incineration Plant	2.62 ± 1.85	
	Soils surrounding the tailings	Sb processing plant	1654.462	Zhou et al. (2020)
	Water Samples	Ore concentrate tank	2.168	
		Filter tank	4.415	
		Tailing tank	2.780	
		Tailing reservoir	3.414	
	Soil	Mining dump site	1267.20	Zhou et al. (2019)
	Soil	Mining soil	248–6946.00	Fu et al. (2016)
	Water	Mining water	0.0067–0.156	
France	Soil	Mining site	691–1986.00	Elbaz-Poulichet et al. (2020)
Germany	Urban soil	Roadside soil	1.75	Thestorf and Makki, (2021)
		Forest topsoil	0.54	
Italy	Soil	Abandoned mine	19–4400	Cidu et al. (2014)
	pore-water		23–1700	
	slag material		0.030	
	runoff		0.8–0.000760 E-6	
Korea	Soil	Active firing range	67.48	Ahmad et al. (2014)
Macedonia	Soi/sediment	Former As-Sb mining sites	37.00	Alderton et al. (2014)
Mongolia	Soil	Coal	55.20	Qi et al. (2008)
Nigeria	Groundwater	Shallow wells (average)	13.5 ± 15.0 to 33.2 ± 36.8 E-6	Etim, (2017)
		Residential	0–76.0 E-6	
		Commercial Area	43.0–64.0 E-6	
		Industrial	52.0–64.0 E-6	
		Agricultural	51.0–66.0 E-6	
Norway	Groundwater	Small arms shooting ranges	~50	Wersin, et al. (2002)
	Runoff	Small arms shooting ranges	5–20	Stromseng et al. (2009)
	Topsoil	Small arms shooting ranges	830	Mariussen et al. (2017)
	Discharge water		0.065	
	Pore-water		19–349	

(continued on next page)

Table 1 (*continued*)

Country	*Media*	*Source of contamination*	*Concentration level (Soil-mg kg^{-1}) and (Water-mg L^{-1})*	*Reference*
Poland	Soil	Historical mining area	0.03–499	Lewińska and Karczewska, (2019)
		Copper Industry	0.12–2.59	
		Shooting Range	10.7–17.0	
		Landfills	0.33–1.55	
	Soil	Former mining sites	12.8–163.00	Lewińska et al. (2018)
Slovakia	Soil	Abandoned Sb mines	9861.00	Hiller et al. (2012)
	Water	Abandoned Sb mines	9.30	
Vietnam	Soil	The Mau Due mine	47–95.00	Cappuyns et al. (2021)
Spain	Soil	Mining	14.3–1,090	Murciego et al. (2007)
Scotland	Soil	Upper Spoil	47.77 ± 16.07	Mbadugha et al. (2020)
		Lower Spoil	27.05 ± 5.44	
		Processing	531.47 ± 326.72	
		Surrounding mine	3.66 ± 0.54	
		Burn	3.51 ± 0.99	
		Gully	1.73 ± 0.04	

(Protano and Nannoni, 2018). Mbadugha et al. (2020) noted that this pollution is of concern, when crops are grown on the land. Abad-Valle et al. (2018) reported that pasture plants and agricultural crops accumulate unsafe levels of heavy metals on polluted mine soils.

Mbadugha et al. (2020) investigated As and Sb levels in surface water and soils near a derelict Sb mine (Louisa mine) in Glendinning, Scotland. They collected 40 soil samples distributed across the study area targeting seven upper spoil heaps, 14 lower spoil heaps, four ore-processing areas, 12 surrounding soils, and three samples located at different depths in the shaft to evaluate the environmental impacts of mining practices on As and Sb levels. The environmental Sb concentration in soils near the Louisa mining site was up to 40 mg kg^{-1}, which was higher relative to < 0.5 to 30 mg kg^{-1} in European soils (Gallagher et al., 1983). High Sb levels were associated with the ore-processing area (i.e., 531.47 ± 326.72 mg kg $^{-1}$), and found in the region where stibnite-containing ores were processed (Protano and Nannoni, 2018). Levels of Sb diminished with distance from mining and processing zones (i.e., upper spoil had 47.77 ± 16.07 mg kg^{-1}, lower spoil had 27.05 ± 5.44 mg kg^{-1}; and locations surrounding the mine had 3.66 ± 0.54 mg kg $^{-1}$). The water samples from the Gully and Glenshanna Burn sites had 1.73 ± 0.04 µg L^{-1} and 3.51 ± 0.99 µg L^{-1} dissolved Sb, respectively, much lower than that at a former Sb mine in Scotland (783 µg L^{-1}) (Macgregor et al., 2015); nevertheless, the concentrations were significantly greater than that in unimpacted freshwater (<1 µg L^{-1}).

Sb production in Australia accounts for nearly two percent of the global share (Red River Resources Ltd, 2020). The Hillgrove mineral field located in the upper Macleay River catchment of northern New South Wales (Australia) has produced over 60,000 tons of stibnite concentrates (i.e., Sb mineral) and gold (Au) (Wilson et al., 2014). Historical mining activity at the Hillgrove mineral field commenced in 1857, ceased in 1921, and recommenced in 1969 (Red River Resources Ltd, 2020). The Hillgrove mineral field was put on care and maintenance in 2016 owing to persistent low Sb prices; it was set to recommence operations by the end of 2020 (Red River Resources Ltd, 2020). Historically poor mine waste management activities have led to the dispersal of Sb-polluted sediments to the coastal floodplain at Kempsey, within 300 km of townships with high population density and intense land use (Ashley et al., 2007). Over 90% of the floodplain exhibits Sb concentrations above background levels, and the area has above the Australian ecological-investigation values (Tighe et al., 2005). It is a leading anthropogenic source for Sb in Australia (Wilson et al., 2014). Thus, Sb uptake in food crops grown in the region and the resulting human exposure through food-chain transfer is of serious concern.

Sb contamination of groundwater can result from various geogenic sources (i.e., chemical and biological weathering of parent materials, leaching, and wet deposition) or anthropogenic sources (i.e., mining, industrial effluents, and pesticide application) (Etim, 2017). In groundwater, Sb exists mainly in inorganic forms, either in trivalent (Sb (III)) or pentavalent (Sb(V)) species (Etim, 2017). Under varying pH of the media and the available forms of Sb, it may undergo either oxidation or reduction reactions. Soluble forms of Sb tend to travel with water. However, less soluble forms are sorbed onto the surface of clay or soil fragments. Sb can leach from landfills (Intrakamhaeng et al., 2020) and sewage sludge (Campos et al., 2019) into groundwater, surface water, and sediment. Sb leached into sediments can be released into the environment via microbial action and distributed via various processes, as discussed below in detail.

3. Distribution and speciation of Sb in the environment

The occurrence of Sb in different environmental media such as soil, water, and sediments, and its toxicity issues have gained increased attention from both public and the scientific community (Herath et al., 2017; Li et al., 2018b; Zhu et al., 2020). As Sb toxicity depends on its distribution and speciation in such environments, it is crucial to understand these aspects to reduce adverse impacts to ecosystems and human health.

3.1. *Distribution in soil*

Sb released into soils is naturally retained by aluminum (Al)-, iron (Fe)-, and manganese (Mn)-oxide, while the soluble antimonate exists primarily as Sb(V) in oxidized and alkaline conditions (Ji et al., 2017). Metal(loid) including Sb mobilization in soils depends on multiple factors such as mineral precipitation–dissolution, adsorption–desorption and ion exchange, complexation, pH, Eh, biotransformation transformation, phytostabilization/uptake and leaching (Palansooriya et al., 2020; El-Naggar et al., 2019; El-Naggar et al., 2018). Background and average values of Sb in soils were reported at 0.3–8.6 mg kg^{-1} and 1 mg kg^{-1}, respectively, while that in parent rocks was < 1 mg kg^{-1} (Johnson et al., 2005). However, significantly high Sb concentrations in soil (up to 4,400 mg kg^{-1}) and soil pore water (up to 1,700 µg L^{-1}) samples were reported in an abandoned mine soil (Cidu et al., 2014). The Sb concentration in soils at abandoned mine sites of New South Wales, Australia, was up to 39.4 mg kg^{-1} (Tighe et al., 2005) (Table 2).

The total Sb level in agricultural soils of Spain near an As-Pb-Sb composite (used for lithium-ion battery applications) dumping site was 14.1–324 mg kg^{-1} (Alvarez-Ayuso et al., 2012), exceeding the highest acceptable limits of Sb in soils recommended by USEPA. Apart from the shooting-range soils analyzed in Norway, several other soils from shooting ranges have been investigated to determine Sb concentration (Table 2) because, as stated, Sb constitutes 2–8% w/w in bullets (He et al., 2019a). In a shooting range in Switzerland, the Sb concentration ranged from 35.0 to 17,500.0 mg kg^{-1} in the surface soil layer (Johnson et al., 2005). The highest Sb concentration at a military training field in Canada was 570.0 mg kg^{-1} (Laporte-Saumure et al., 2011) whereas that in the topsoil from a study in Norway was 830.0 mg kg^{-1} (Mariussen et al., 2017).

3.2. *Distribution in the aquatic environment*

Sb occurs naturally at low concentrations in unpolluted, natural water bodies. Depending on the physicochemical environmental setting and geographical positioning, the concentration of total dissolved Sb in

Table 2
Distribution of Sb in soil and aquatic environments.

Region/ country	Source/site	Species	Concentration (soil-mg kg^{-1}) and (water- µg L^{-1})	Reference
New South, Australia	Mining area Soil	Sb (total)	39.40	Tighe et al. (2005)
Xishan, China	Mining area Soil	Sb (total)	5949.20	Qi et al. (2011)
Iran	Agricultural soil	Sb (total)	2.50	Mohammadpour et al. (2016)
China	Mining area soil	Sb (total)	547.00	Couto et al. (2015)
China	Mining area soil	Sb(III) and (V)	229–1472.00	Wei et al. (2015)
China	Mining area soil	Sb (total)	267–5536.00	Ning et al. (2015)
Australia	Wetland soil	Sb (total)	22000.00	Warnken et al. (2017)
Australia	Sb processing industry soil	Sb (total)	7900.00	Ngo et al. (2016)
Italy	Mining area soil	Sb (total)	4400.00	Cidu et al. (2014)
Italy	Mining area soil	Sb (total)	23–5140.00	Armiento et al. (2017)
Xikuangshan, China	Mining area soil	Sb (total)	3061.00	Li et al. (2014)
Australia	Dumping area soil	Sb (total)	4517.00	Wilson et al. (2013)
Australia	Mining area soil	Sb (total)	2735.00	Wilson et al. (2013)
Spain	Agricultural soil	Sb (total)	14.1–324.00	Alvarez-Ayuso et al. (2012)
Spain	Mining area soil	Sb (total)	35.00	Pérez-Sirvent et al. (2012)
Spain	Mining area soil	Sb (total)	5–40.00	Pérez-Sirvent et al. (2011)
Czech Republic	Forest soil	Sb (total)	379.00	Ettler et al. (2010)
Czech Republic	Agricultural soil	Sb (total)	3.1–131.00	Ettler et al. (2010)
Switzerland	Shooting field soil	Sb(III) and (V)	21.00	Wan et al. (2013)
Switzerland	Shooting field soil	Sb (total)	21.00	Conesa et al. (2011)
Cologne, Germany	Roadside soil	Sb (total)	6.19	Földi et al. (2018)
Xikuangshan, China	Mining area soil	Sb(III) and (V)	11798.00	Okkenhaug et al. (2011)
Lengshuijiang, China	Dumping area soil	Sb (total)	5949.20	Qi et al. (2011)
Xikuangshan, China	Mining and smelting soil	Sb (total)	5045.00	He, (2007)
Scotland	Mining area soil	Sb (total)	10–1200.00	Gal et al. (2007)
Spain	Mining area soil	Sb (total)	225–2450.00	Murciego et al. (2007)
Japan	Smelting industry soil	Sb(V)	2900.00	Takaoka et al. (2005)
Switzerland	Shooting field soil	Sb(V)	35–17500.00	Johnson et al. (2005)
China	Soil	Sb (total)	2.535	Geng et al. (2020)
Mau Due mine, North Vietnam	Soil	Sb (total)	31–91.00	Cappuyns and Campen, (2020)
Erme, south west England	Sediment-plastic mixtures	Sb (total)	256–47600.00	James and Turner, (2020)
Mau Due mine, North Vietnam	Mining wastes (e.g., slags)	Sb (total)	186–27221.00	Cappuyns and Campen, (2020)
Italy	Mining area surface water	Sb (total)	0.5–148	Armiento et al. (2017)
Mexico	River water Groundwater	Sb(total	1.2–220.60	Baeza et al. (2010) Wu et al. (2011b)
Yangtze River, China		Sb(III) and (V)	0.023–0.116, 0.047–0.441	
Finland	Groundwater	Sb (total)	0.02–0.82	Lahermo et al. (2002)
Ethiopia	Groundwater	Sb (total)	0.002–1.780	Reimann et al. (2003)
Yunnan Sichuan Province, China	Geothermal waters	Sb (total)	0.23–173.00	Guo et al. (2020)

surface- and ground-water varies from ng L^{-1} to mg L^{-1} (Long et al., 2020b). The average Sb concentration is typically < 1.0 mg L^{-1} in untapped natural water (Filella et al., 2002). In recent years, the occurrence of various chemical species of Sb in aquatic systems has been acknowledged (He et al., 2019b; Long et al., 2020b; Li et al., 2018a). Mining activities influence the Sb concentration in soils and natural waters (Long et al., 2020b). The analysis of water samples collected from the Sb-mining site in Xikuangshan (People's Republic of China) revealed 2.0–6,384 µg L^{-1} oxidized Sb concentrate, considerably higher than the average global Sb concentration (1 µg L^{-1}) (Wang et al., 2011). Of 18 samples taken from the Xikuangshan mining site, the most prevalent Sb species detected was Sb(V), with small Sb(III) concentrations found in four samples (Liu et al., 2010). The drinking water samples collected from the Xikuangshan mine, China, contained 53.6 ± 46.7 µg Sb L^{-1} (Fu et al., 2010). Sharifi et al. (2016) studied Sb content and its flow dynamics in water. The authors proposed that the oxides and hydroxides of ferric iron are the most suitable for Sb reduction via adsorption or co-precipitation which is in agreement with Baeza et al. (2010).

Field trial studies have shown that Sb(III) and Sb(V) contents decrease via dilution, and further their dissolved phase are separate out during downstream movement of the Sb. Resongles et al. (2013) carried out a pH-gradient and oxygen-concentration dependent speciation investigation of suspended Sb particulates in Carnoules mine water (southern France). The results showed that 70–100% of Sb particulates belonged to Sb(III), and $< 30\%$ Sb belonged to Sb(V). Future studies need to consider the effects of unpredictable weather conditions on the distribution of Sb in contaminated sites, particularly from mine sites. For illustration, intense rainfalls alter Sb distribution in environmental compartments, by increasing the Sb level in oceans via rivers and sediment transport off agricultural fields (Armiento et al., 2017). Alderton et al. (2014) reported that surface-water samples contained more Sb (average 0.6–2.1 µg L^{-1}) than groundwater samples. Similarly, variation was reported among surface and bottom layers of fresh waters. Wu et al. (2011b) compared the key species of soluble Sb in the estuary of the Yangtze River with a nearby freshwater site. The findings showed that Sb(V) and Sb(III) levels in surface waters ranged from 0.121 to 0.567 µg L^{-1} and 0.029–0.736 µg L^{-1}, respectively. The bottom layer had the lowest concentrations of Sb(V) (0.047–0.441 µg L^{-1}) and Sb(III) (0.023–0.116 µg L^{-1}). Comparable results have been documented by others (Asaoka et al., 2012; Jabłońska-Czapla et al., 2015).

3.3. Chemical forms and speciation

The Sb concentration in the environment is dependent on the soil redox potential (Eh), pH, the presence and content of Fe- and Mn-containing ores or minerals, soil cation exchange capacity, humic acids (HAs), and dissolved organic matter (DOM) (Herath et al., 2017; Rinklebe et al., 2020). In soil and sediment, oxide and hydroxides of Fe and Mn play key roles in the adsorption of Sb, particularly Sb(III). For example, Fe and Mn accelerate the oxidation rate of Sb(III) to Sb(V) and change the concentration of both the species (Xu et al., 2011). However, soluble Sb compounds usually persists in four distinct chemical states [Sb(-III)/Sb(0)/Sb(III)/Sb(V)] (Moreno-Andrade et al., 2020; Li et al., 2018b). The chemical states of Sb determine its transformation, mobilization, and immobilization. Sb(III) has a lower solubility and mobility than Sb(V) (Johnson et al., 2005; Wu et al., 2011b). Although Sb(III) has lower water solubility than Sb(V), the former has a stronger affinity towards Fe and Mn hydroxides, and HAs in terrestrial systems (Liu et al., 2015). *Generally, compared to Sb(III), higher Sb(V) concentrations* occur in natural aquatic environments (Wilson et al., 2010; Filella et al., 2002; Fu et al., 2016). Aquatic Sb concentrations are influenced by Sb sorption mechanisms, Sb mobilization or immobilization, pH, Eh, co-occurring metals ions, and DOM (Frohne et al., 2011; Herath et al., 2017; Rinklebe et al., 2020). Natural organic matter may also regulate aqueous phase Sb concentrations (Filella and May 2005; Filella and Williams. 2012). Buschmann and Sigg, (2004) showed that Sb(III) was *bound via carboxylic and phenolic groups. >30% of overall Sb(III) can* be bound with aquatic HAs, and the process is strongly influenced by low ionic strengths of the media (Nakamaru and Peinado, 2017).

Furthermore, the pH of a specific medium has a critical role to play in Sb speciation in that medium. In the pH range of 1.0–11.0, Sb(III) generally occurs in its hydroxide form such as $Sb(OH)_3$, SbO(OH), and $HSbO_2$, whereas under extreme, low pH (<1.0), Sb(III) persists in the cationic form $SbO^+/Sb(OH)_2{}^+$ (Bergmann and Koparal, 2007). At higher *pH (>11.0), the predominant Sb(III) forms exist as anions* $SbO_2{}^-$ *or Sb* $(OH)_4{}^-$. In the pH range of 1.0–14.0, $Sb(OH)_6{}^-$ is the dominant form of Sb(V), while at the lowest pH (<1), Sb(V) primary exists in the $SbO_2{}^+$ form (Long et al., 2020b). Sb(V) was found to be predominant and exists in the form of $Sb(OH)_6{}^-$ in the drainage water samples collected from the Xikuangshan Sb mine, China (Liu et al., 2010).

Computational modeling predicted that, in anaerobic water at pH ranges from 1.4 to 11.8, the Sb(III) form exists as the hydroxy complex ($Sb(OH)_3$). However, under aerobic, aquatic conditions, the negatively charged ($Sb(OH)_6{}^-$) is the predominant species of Sb(V) when pH > 2.7 (Filella and May 2003). Nevertheless, in anaerobic and aerobic waters, both forms [Sb(III), Sb(V)] exist (Filella et al., 2002), and this is ascribed to microbial activities, chemical-facilitated changes in Sb(III) – Sb(V) in anaerobic waters, or mixing with concurring waters (Kulp et al., 2014; Li et al., 2013). Sb(III) oxidation, facilitated by Fe and Mn, is controlled by several ores or minerals and trace metals present in natural environments (Lenz et al., 2006; Multani et al., 2016). Sb(III) oxidation using hydrogen peroxide (H_2O_2) was studied under measured environmental concentrations of Pb^{2+}, Zn^{2+}, Cu^{2+}, and Mn^{2+} (Elleouet et al., 2005). The results revealed that the presence of trace elements enhanced the reaction kinetics over a wide-ranging pH. Some microorganisms are able to transform Sb(III) and Sb(V) forms into several organic and inorganic compounds via diverse mechanisms, such as fluxion in concentrations of Sb(III), oxidation and reduction of Sb(III) and Sb(V), respectively, and methylation of Sb(III) (Filella et al., 2007; Li et al., 2016). Lehr et al. (2007) showed Sb(III) oxidation using wild and mutant varieties of *Agrobacterium tumefaciens*. In anaerobic water sediments, Kulp et al. (2014) showed bacteria-mediated Sb(V) reduction via a respiratory route using lactate and acetate as energy sources. However, microbe-assisted Sb oxidation is in its infancy and needs more research to understand the mechanisms involved (Li et al., 2013).

4. Biogeochemical processes of Sb in the environment

The global biogeochemical cycle for Sb is poorly documented in comparison to other elements in the literature. Some studies have attempted to describe the atmospheric emissions of Sb (Fort et al., 2016; Iijima et al., 2008; Tian et al., 2011; Tian et al., 2014); however, the transformation pathways and quantities of Sb among different environmental compartments (e.g., soil, aquatic bodies, biota, and atmosphere) have not been well defined. Additional information about the dispersal and speciation of Sb in the natural environment is necessary in assisting scientists to fill this gap. Meanwhile, an up-to-date understanding of different biogeochemical processes of Sb in soil and aquatic environments is essential, which is described in this section (Fig. 3).

4.1. Biogeochemical processes of Sb in the soil

Soil characteristics highly influence the biogeochemical processes of Sb (Constantino et al., 2018; Frohne et al., 2011; Natasha et al., 2019; Rinklebe et al., 2020), which in turn determine Sb speciation, retention versus mobility in soil, plant uptake, and transfer to the water environment (Herath et al., 2017). Such biogeochemical processes include adsorption–desorption, dissolution, leaching, (co)precipitation, redox transformations, and interactions of Sb with microorganisms (Fan et al., 2020; Natasha et al., 2019; Zhu et al., 2020).

The adsorption process is a major retention mechanism for Sb in soil. Sb is adsorbed by different soil constituents, including clay minerals and other inorganic adsorbents and organic adsorbents. For instance, clay minerals, such as montmorillonite, have a high adsorption capacity for Sb (Kabata-Pendias, 2011). The weathering of clay minerals and breaking of their edges stimulate the adsorption of Sb onto clay mineral surfaces (Herath et al., 2017; Natasha et al., 2019).

Inorganic adsorbents, such as Fe-, Mn-, and Al-(hydr)oxides (also constituents of soil clays e.g., layered-aluminosilicate clay minerals) affect Sb adsorption in soil. Minerals like hematite, ferrihydrite, and goethite contain Fe-oxides, which participate in immobilizing Sb in soil. As a result, several studies have attempted to use Fe-based adsorbents to remediate of soils contaminated with Sb. For instance, goethite adsorbed Sb(III) over a pH range from 3 to 12, and Sb(V) at pH < 7 (Filella and Williams, 2012). Zero-valent, Fe-functionalized-carbon nanotubes is a competent adsorbent material for Sb(III) and Sb(V) (Mishra et al., 2016). In particular, the authors showed high adsorption of Sb(III) (250 mg g^{-1}), which was attributed to the high surface area of nano-zero-valent Fe particles. Naturally occurring Mn oxides (birnessite) and Al oxides (gibbsite) and their hydroxides, are common minerals in soils. Mn and Al oxihydroxides can interact with Sb(III) and Sb(V), and reduce Sb mobility in agricultural soils. Belzile et al. (2001) described the oxidation mechanism of Sb(III) by Mn oxides under anaerobic conditions as follows:

$$\mathrm{MnO}_{2(S)} + \mathrm{Sb(OH)}_{3(aq)} + H_2O_{(l)} \rightarrow \mathrm{Mn(OH)}_{2(aq)} + H_3\mathrm{SbO}_{4(aq)} \tag{1}$$

MnO_2 is more capable of oxidizing Sb(III) than Fe (hydr)oxides (Belzile et al., 2001; He et al., 2019b). A combination of Fe-Mn oxide materials showed greater adsorption capacity for Sb(III) than Fe (hydr) oxides alone (1.76 mmol g^{-1} vs. 0.83 mmol g^{-1}). Sb(III) oxidation to Sb (V) by Mn oxides, which facilitated Sb(V) adsorption by Fe (hydr)oxides, was the underlying mechanism (Xu et al., 2011). Direct adsorption of Sb (V) by Mn (hydr)oxides, however, is not yet well documented. Sb(V) adsorption on surfaces of gibbsite was described (Eq. II and III) by He et al. (2019b):

$$\mathrm{Al} - OH_{(S)} + H^{+}_{6(aq)} \leftrightarrow \mathrm{Al} - \mathrm{(OH)}^{+}_{2(S)} \tag{2}$$

$$2\mathrm{Al} - OH_{(S)} + \mathrm{Sb(OH)}^{-}_{6(aq)} \rightarrow \mathrm{(AlO)}_2 Sb\mathrm{(OH)}^{-}_{4(S)} + 2\mathrm{H}_2O_{(l)} \tag{3}$$

The surface charge of Al oxides will become prevalently positive in acidic environments (Kosmulski, 2009), which stimulates electrostatic forces that interact with anionic forms of Sb(V) (He et al., 2019b; Xu et al., 2001). Regarding Sb(III) adsorption, (hydr)oxides of Fe and Al have a lower adsorption capacity than Mn (hydr)oxides. However, due to the higher abundance of (hydr)oxides of Fe and Al in soil than Mn (hydr)oxides, the former usually govern the behavior of Sb(III) (Wilson et al., 2010).

Sb adsorption is also influenced by soil organic matter (SOM) (Inam et al., 2019). Soil HAs accommodated a considerable amount of Sb(III) (up to 34% of total soil Sb level) (Buschmann and Sigg, 2004; Ettler et al., 2007; Tserenpil and Liu, 2011), demonstrating a high affinity

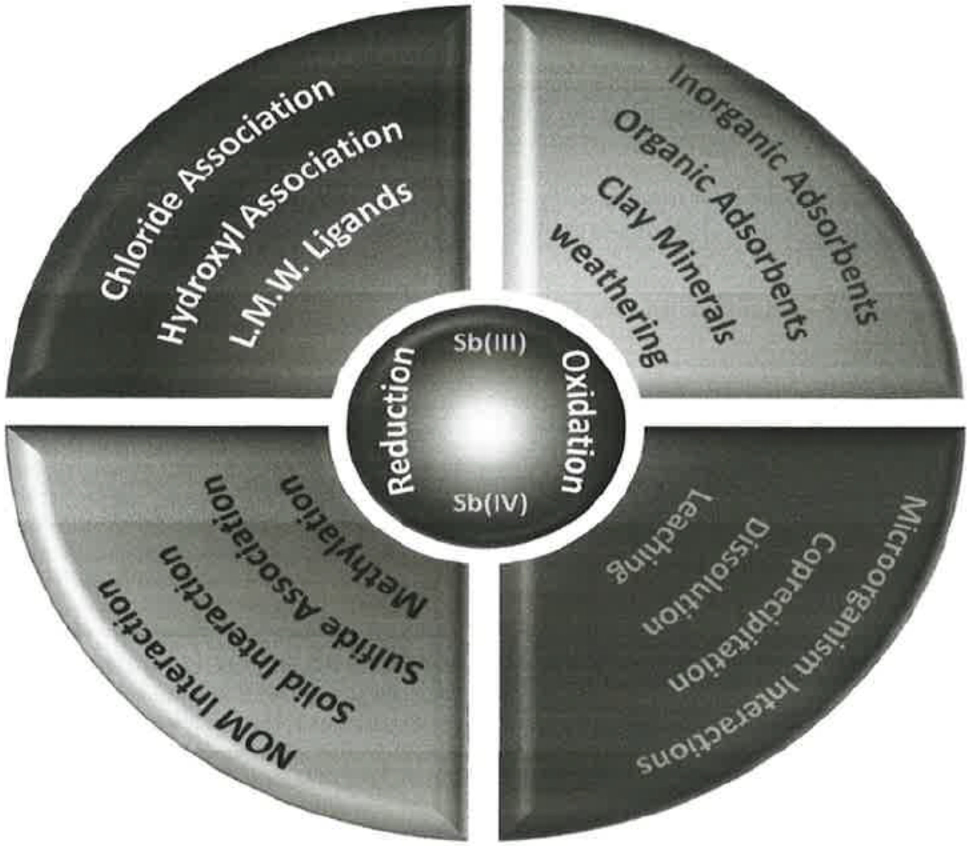

Fig. 3. Factors affecting biogeochemical processes of Sb in soil and water environments. (NOM: natural organic matter; LMW: low molecular weight).

between Sb(III) and SOM. The postulated complexation mechanisms of Sb(III) with functional groups of OM were described by Wilson et al. (2010), including the generation of anionic Sb complexes with carboxy groups and ligand substitution with the Sb-center. HAs can also stimulate Sb(III) oxidation to Sb(V). Humic substances were reported to adsorb more Sb(III) than Sb(V) (Inam et al., 2019); however, the underlying mechanism explaining this disparity is not yet well documented, and further investigations are required in this aspect (Wilson et al., 2010).

Other biogeochemical processes of Sb in soil include the dissolution and leaching of Sb from Sb-bearing primary minerals (e.g., Sb_2O_3 and Sb_2S_3) and co-existence of Sb(III) and Sb(V) forms in soil (Cappuyns et al., 2021; Herath et al., 2017; Shan et al., 2020). A recent study in Vietnam found that wastes at the Mau Due Sb mine, where the primary Sb mineral was stibnite (Sb_2S_3), leached up to 1.7% of its total Sb content (191–15,699 mg kg^{-1}) to water, and the Sb release increased at a pH range 7.5–12.8 (Cappuyns et al., 2021). Several factors were reported to accelerate the dissolution and leaching processes of Sb, including photo-irradiation, low-molecular-weight-dissolved organic acids, total SOM content, sulfur oxidation, soil pH, and soil Eh (Frohne et al., 2011; Fu et al., 2016; He et al., 2019b; Rinklebe et al., 2020; Shan et al., 2020). Dissolution of Sb is always associated with dynamic alteration in soil biogeochemical conditions, enhancing its mobility in soil and facilitating Sb translocation from the soil profile into water bodies. For instance, soil under flooded, anaerobic conditions commonly has a high dissolution rate of Fe oxides, accompanied by the release of DOM (Rinklebe et al., 2016; Shaheen et al., 2014). Consequently, flooding conditions can induce dissolution of Sb-Fe oxides minerals and Ca-antimonate (Rinklebe et al., 2020; Zhu et al., 2020). Additionally, the dissolution of dissolved organic carbon under flooded condition can result in increased Sb release owing to the strong Sb-organic molecule association. However, soil flooding can also accelerate the adsorption of Sb due to Sb(V) reduction to Sb(III), which has higher affinity to SOM (Grob et al., 2018). These contrasting results are mainly attributed to the variable conditions of soil pH, site-abundant soil minerals including Fe and Al oxides, and the induced changes of soil Eh, levels of soil-dissolved organic carbon, and sulfur chemistry.

(Co)precipitation of Sb may also occur in soil via binding of Sb with compounds of amorphous hydroxides and Ca (Ranđelović et al., 2020; Wilson et al., 2010). Sequential dissolution and re-precipitation of Sb $(OH)_3$ reportedly controlled Sb availability in soil surrounding a mine site in Vietnam (Cappuyns et al., 2021). However, (co)precipitation of Sb can only have a major role when soil Sb concentration is elevated to a level that allows the (co)precipitation process. It is supposed to have a marginal role in soils with low total Sb concentration. In soils with low total Sb concentration, adsorption–desorption processes are the major mechanisms for immobilization of Sb (Herath et al., 2017). The biogeochemical processes of Sb also can be affected by interactions between soil microorganisms and Sb. For instance, arbuscular mycorrhizal fungi, bacteria, and archaea can induce changes in Sb speciation and bioavailability in soils, thereby affecting plant uptake of Sb (Girolkar et al., 2021; Wei et al., 2016). Similarly, Fe- and S-oxidizing and reducing bacterial species are likely to impact Sb transformations in soil. The interactions between Sb and soil microorganisms are discussed in detail in Section 5.

4.2. *Biogeochemical processes of Sb in aquatic environments*

Biogeochemistry of Sb in aquatic systems has been rarely studied, and this field lacks sufficient experimental data (Fu et al., 2016). In aqueous solution, Sb can form complexes with low-molecular-weight ligands and interact with colloidal and solid phases of inorganic or organic substances; these processes can be affected by living organisms (Filella and Williams, 2012; Sun et al., 2017). Sb(III) and Sb(V) can readily hydrolyze in aquatic systems, particularly under alkaline conditions, while Sb species are more stable in acidic solutions (Filella and

Williams, 2012). Interactions of Sb with low-molecular-weight ligands, such as hydroxyl, chloride, sulfides, and organic substances, vary widely according to the pH of aqueous solutions. For instance, SbO_2^+ dominates under acidic conditions, but, when the solution pH turns to be neutral or alkaline, Sb can interact with hydroxyls to form $Sb(OH)_6^-$ as the predominant species (Filella et al., 2002; He et al., 2019b; Herath et al., 2017). In terms of Sb interactions with chloride, limited data are available. It is not yet evident whether chloride or hydroxy-chloride containing forms of Sb(III) and Sb(V) are formed in seawater.

Under an oxic environment, Sb(V) is the abundant form in solution, while Sb(III) is the common form under anoxic conditions. Sb can interact with sulfur under anoxic conditions, forming both soluble (e.g., SbS_2^{2-}) and/or insoluble (e.g., $Sb_2S_{3(s)}$) species, which is dependent on pH of the system (Filella et al., 2002; Polack et al., 2009). Interactions of Sb with organic ligands having O-bearing functional groups, such as alcohols, phenols, and carboxylic acids, also have an important role in Sb mobility in aquatic environments (Dousova et al., 2015). He et al. (2019b) reported that up to 85% of total Sb in lake water was complexed with organic substances, such as fulvic and HAs. In aqueous solutions, Sb (III) can be associated with carboxylic and hydroxy carboxylic acid functional groups within a pH range between 3 and 9 (Tella and Pokrovski, 2009). However, the binding of Sb(V) by organic ligands is not well documented.

Understanding the biogeochemical processes of Sb in water would allow the application of suitable amendments to reduce the toxicity of Sb to living organisms. Manganese oxides can be efficient in the immobilization of Sb(III) in water environments under anoxic conditions via adsorption and oxidation mechanisms (He et al., 2019b). However, compared to other toxic elements, Sb has received much less attention in research that elucidates detailed biogeochemical processes and mechanisms and water remediation techniques.

In conclusion, various factors affect the biogeochemical processes of Sb in soil and water, as discussed previously in this review and represented in (Fig. 3). Therefore, future research is warranted to ascertain Sb interactions with solid phases and natural OM, speciation of methylated Sb, and induced biogeochemical changes in Sb species under different oxic-anoxic conditions in soil and water environments.

5. Bioavailability and toxicity of Sb to biota

Due to its toxicological nature, Sb contamination and translocation through the ecosystem can pose severe threats to biota and human health. To assess the potential risks, regulatory guidelines based on total metalloid concentration in soils are commonly used (Greenberg et al., 2014). However, binding with Fe and Mn oxides, adsorption, precipitation, and complexation in soil solution may hinder the mobility of Sb and other metalloids. Thus, the assessment based on total metal(loid) concentration including Sb may overestimate of the potential risks (Bagherifam et al., 2019b; Bolan et al., 2008). Therefore, considering the dynamic process of bioavailability is important.

5.1. *Bioavailability of Sb*

To be bioavailable, Sb must be in its mobile form and should be readily available for biological uptake to pose a risk on target organs (Kuppusamy et al., 2017). Water-soluble Sb can be readily available for plant uptake, and excessive accumulation can lead to toxic effects (Corrales et al., 2014; Tschan et al., 2010). The bioavailability of Sb in the soil environment is mainly governed by several factors as represented in (Fig. 4). A plot scale study by Zhong et al. (2020) revealed that Sb is more easily adsorbed by plant roots in alkaline soil (pH 8.39) than acidic soil (pH 4.91). Moreover, the bioavailability of Sb increases when soil Eh decreases (Zhu et al., 2020). Management practices also affect Sb bioavailability. For instance, prolonged flooded conditions, which are required for paddy cultivation, cause favorable conditions for excessive Sb uptake by plants (Zhu et al., 2020).

Nakamaru and Peinado (2017) reported that Sb availability to plants could increase by 2–4 times by increasing SOM content. Sb bioavailability is also influenced by the presence of ions (PO_4^{3-}, NO_3^-, CO_3^{2-}, and SO_4^{2-}) via competitive adsorption and co-precipitation (Zhu et al., 2020). Associated dissolution of Fe and Mn (hydr)oxides can also increase Sb bioavailability. Wan et al. (2013) reported decreased available Sb levels initially with flooded conditions due to increased proportion of Sb(III) under reduced conditions, but subsequently increased owing to the dissolution of Fe and Mn oxides. This resulted in a 10-fold increment in shoot Sb level of *Lolium perenne* L. (perennial ryegrass) but an 80% decrease in *Holcus lanatus* L. The results indicate the importance of the influence of oxidation state and species on Sb uptake. The presence of NO_3^- in soil may inhibit the reductive dissolution of Fe minerals, thus lowering the bioavailability of Sb in paddy soils (Zhang et al., 2021b). Soil microorganisms, such as bacteria, archaea, and fungi, can mediate the bioavailability of Sb by inducing speciation changes (Li et al., 2016; Long et al., 2020a). For example, inoculation of plant roots with fungal species of *arbuscular mycorrhizas* could promote Sb uptake (Pierart et al., 2015; Wei et al., 2016).

Most plants have a higher affinity for absorbing Sb(III) than Sb(V) (Huang et al., 2012; Ji et al., 2017; Ren et al., 2014). Several methods are deployed for determining Sb availability in soil, such as Sb measurement in pore water, one-step- or successive-extraction methods (Bagherifam et al., 2019b), and the thin-film-diffusion-gradient technique (DGT) (Luo et al., 2010). Compared to total Sb in soil, low levels of water-soluble Sb were found in Sb-contaminated soil in Germany (0.5%) (Lintschinger et al., 1997), the United Kingdom (<1%) (Flynn et al., 2003), and Jiangxi Province, People's Republic of China (0.52–3.51%) (Liu et al., 2007), which confirm its low bioavailability.

An *in vivo* test by Denys et al. (2012) showed that the relative bioavailability of Sb varied from 2 to 6% in mining- and smelting-contaminated soil. In the same study, no Sb was detected in biological endpoints of kidney, liver, and bones of humans from the smelter-contaminated soils, implying low bioavailability in terrestrial ecosystems. Several methods are commonly used to determine *in vitro* amounts of bio-accessible Sb concentrations. These methods include the Simplified Bioaccessibility Extraction Test (SBET), the Physiologically Based Extraction Test (PBET), and Unified BARGE Method (UBM) (BARGE is the BioAccessibility Research Group of Europe) (Denys et al., 2012; Li et al., 2014). Sb concentrations were reported ranging from 19 to 60,000 mg kg^{-1} in soil samples from a contaminated mining site at Glendinning, Scotland, UK, with the bio-accessible amount in gastric extraction ranging from 5.05 to 9.11%, as determined by the UBM method (Denys et al., 2012). An average Sb level of 3,061 mg kg^{-1} was reported in soils from the Xikuangshan Sb-mining area, China, with average bio accessibility values of $5.89 \pm 6.44\%$, $7.83 \pm 9.82\%$, $3.03 \pm 3.53\%$ determined by SBET, PBET (gastric), and PBET (intestinal) extraction, respectively (Li et al., 2014). Wilson et al. (2014) reported Sb levels of 0.2–16.6 mg kg^{-1} in the Macleay River Floodplain in northern New South Wales, Australia, with bioaccessibility $< 3\%$, as measured by SBET. Using the UBM test, an investigation on a football field contaminated with mine tailings in France demonstrated Sb bio accessibility of less than detection limits, although the total Sb concentrations ranged from 157 to 363 mg kg^{-1} (Pascaud et al., 2014). Lower bio accessibility of Sb in the intestinal phase (1–28%) than the gastric phase (6–83%) was shown in soils collected from a shooting range in Australia (Sanderson et al., 2012). In most cases, low bio accessibility of Sb in soils can be attributed to entrapment of Sb by Fe oxyhydroxides, the presence of sulfides in soils, or the association of Sb with the residual fraction of soil (Herath et al., 2017). High Sb bioavailability can cause toxicities in animals, plants and humans (He et al., 2019a).

5.2. *Toxicity to plants and microorganisms*

Sb existing in soil solution can be readily taken up by plants, potentially resulting in adverse impacts to the plants (Maresca et al.,

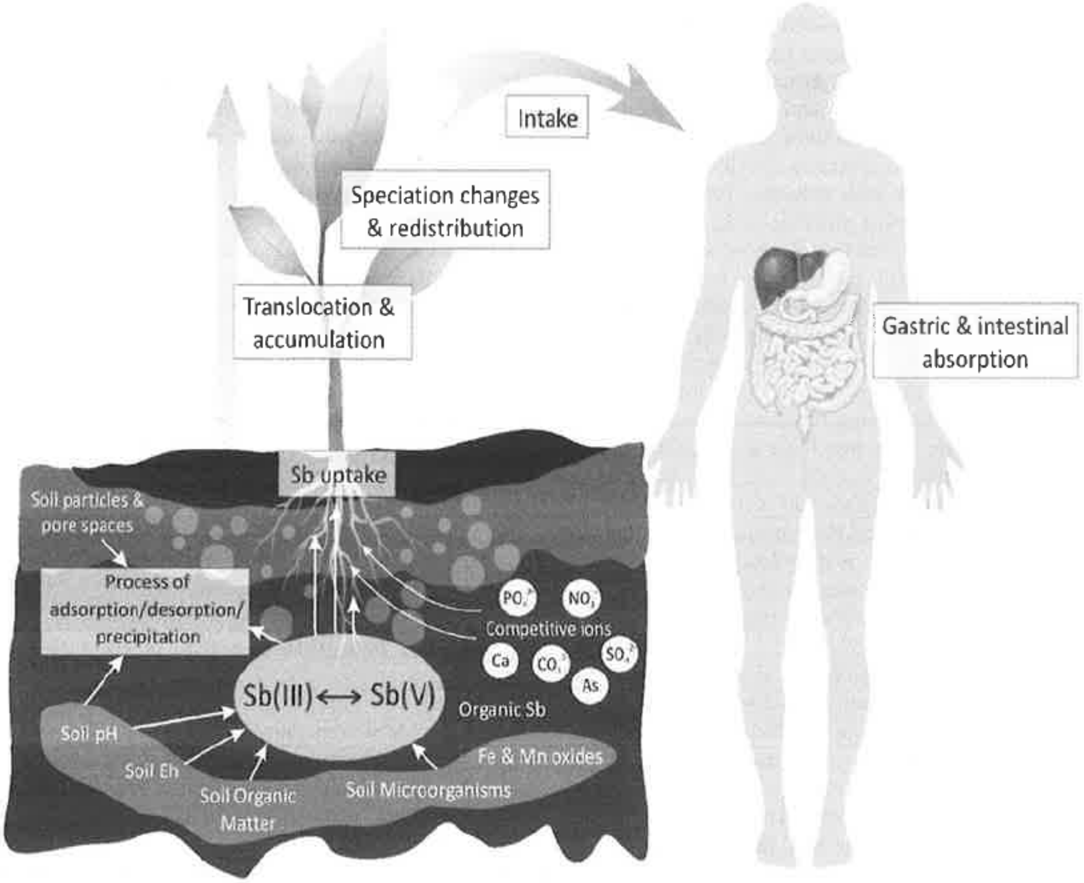

Fig. 4. Schematic representation of the major factors affecting bioavailability and uptake of Sb.

2020). The Sb-associated, plant-toxic effects are growth retardation, repression of photosynthesis, uptake and assimilation of substances that are generally not taken up, and reduced synthesis of some metabolites and hormones (Baek et al., 2014; Feng et al., 2013; Zhou et al., 2018). Zhou et al. (2018) studied *Acorus calamus* (common name: calamus), a tall perennial herb, and observed that both Sb(III) and Sb(V) species adversely affected the synthesis of leaf photosynthetic pigments (i.e., chlorophyll *a* and b and carotenoids), plant height, dry weight, and net photosynthetic rate. Previously, Feng et al. (2016) revealed that the various species of Sb would be alter the morphology of plant roots and adversely impacted development of the root system. Feng et al. (2020) reported that Sb(III) increased the biosynthesis of abscisic acid in rice plants, which can impede cell division, elongation, and growth. Furthermore, various species of Sb persuaded oxidative stress, nevertheless rice crop accelerated the actions of ascorbate peroxidase (APX) and superoxide dismutase (SOD) to counter the oxidative stress. Plant hormone synthesis can also be altered as a result of Sb(III) uptake, affecting root morphology (Zhu et al., 2020). Furthermore, various species of Sb persuaded oxidative stress, nevertheless rice crop accelerated the actions of ascorbate peroxidase (APX) and superoxide dismutase (SOD) to counter the oxidative stress.

Sb toxicities on microorganisms have been well studied and reported. Kataoka et al. (2018) reported a strong selective pressure on As (III)-oxidizing bacterial populations in a soil bacterial community, induced by various Sb species. The same study revealed that the coexistence of Sb with As has an important role on As redox reactions in the environment. Although these toxic effects are present, some microorganisms are capable of remediating Sb in impacted environments (Wang et al., 2011). Various chemical processes of microorganisms enable them to survive in Sb-rich environments (Li et al., 2021), which can be identified as efflux, methylation, Sb(III) oxidation, and Sb(V) reduction (Li et al., 2016). For example, in yeast, the accretion of the lethal, intracellular form of Sb(III) was reduced by preventing its entry into cells or, if it entered cells, its active expulsion. Also, a harmless form could be made inside the cell space (Wysocki et al., 2001). Further, microbial-assisted oxidation of Sb(III) transmuted Sb(III) to its oxidized form (Sb(V)), which is less toxic and more immobilized, thereby assisting bioremediation of Sb-contaminated soil and allowing for its safe disposal (Li et al., 2019).

5.3. *Risk to animals and humans*

Sb is documented as a reckoned oncogenic hazardous contaminant. It displays multifarious compound specific geno and cyto-toxicity and *there is adequate proof to suppose Sb containing compounds to* be a potential human carcinogen. Exposure to Sb or Sb-derived complexes; through dermal, oral, and inhalation, by animals and humans can have grave adverse health impacts (Bagherifam et al., 2019b; Wu et al., 2011a). Sb compounds have an affinity toward thiol groups (i.e., sulfhydryls) of glutathione and proteins. They retained for an extended duration and disturb enzymatic activity, and adversely affecting several organ systems, including lungs, heart, liver, and kidneys (Li et al., 2016; Wang et al., 2018). *An early study showed that inhalation of Sb*(III) oxide leads to lung cancer in female mice (Groth et al., 1986). Baek et al. (2014) studied the response of Asian earthworm (*Perionyx excavates*) exposed to elevated Sb levels. Negative effects on the earthworm's survival and morphological abnormalities (i.e., surface-casting activity) were reported (Baek et al., 2014).

After exposure to Sb, systemic, immunological, neurological, reproductive, genotoxic, and developmental effects and cancer, have been well documented by the United States Public Health Service (US-PHS) (US-PHS, 1992). Sudden-infant-death syndrome (SIDS) is found to be related to the inhalation of toxic gases (e.g., stibines) that originate from methylation of Sb species by the fungus *Scopulariopsis brevicaulis* in polyurethane-foamed crib mattresses (Richardson, 1994). However, studies are also available indicating no causal link to SIDS with Sb biovolatilization (Cullen et al., 2000; Jenkins et al., 2000). A health risk analysis found that the hazard quotient (HQ) values of Sb in vegetables ranged from 1.61 to 3.33 (Zeng et al., 2015). A HQ is defined by dividing the chronic daily intake by the mean reference dose; if HQ value is higher than 1, it appears that there are obvious health risks. In this study, the chronic daily intake was above the safe limit prescribed by the Food and Agriculture Organization (FAO) and WHO. These results indicated that long-term utilization of vegetables from Sb contaminated soils might jeopardize the health of inhabitants near the Xikuangshan mine in Hunan, China (Zeng et al., 2015). However, there are few data existing to justify the adverse impact of Sb contamination and their level of toxicity to human beings as there is always a co-exposure of As as well to the working staffs exposed to Sb during mining and smelting activities (Nishad and Bhaskarapillai, 2021; NTP, 2018). Most of the investigations and research lack adequate size of the sample and appropriate control population, and that make the outcomes inconsistence. However, there are few recent animal investigations and reports revealed the toxicity of Sb to living organisms (Schildroth et al., 2020; Saerens et al., 2019; Agency for Toxic Substances and Disease Registry, Atlanta, 2019).

6. Risk management of Sb in contaminated environments

Both bioavailable and immobilized fractions of Sb are found in the soil matrix. Numerous studies have considered the bioavailable fraction of Sb in soil and found it important (Majzlan et al., 2016; Nakamaru and Peinado, 2017). Therefore, actions need to be taken to manage the bioavailable fraction of Sb in the soil, mainly where agricultural practices are undertaken. However, most experiments that have focused on risk management of Sb in contaminated soils have been restricted to laboratory research, with limited field applications due to several factors (Fig. 5).

6.1. *Immobilization using soil amendments*

The application of materials (e.g., clay minerals, biochar, organic composts, and fly ash) to a metal(loid) including Sb contaminated soil can reduce flow and transport of Sb in the soil and its availability for plants, owing to the strong sorption of such materials (Bolan et al., 2021; Kumar et al., 2020c; Palansooriya et al., 2020). Among various amendments, chemical additives provide the best immobilizing potential compared to others, including biochar (Kumar et al., 2021a; Doherty et al., 2017; Silvani et al., 2019). In some cases, biochar increased Sb mobilization in soil; therefore, the use of biochar needs further consideration before its application in Sb contaminated soils (Hua et al., 2021; Rinklebe et al., 2020).

Several reports have demonstrated the effective immobilization of Sb by ferrous sulfate, which induces Sb(V) reduction to Sb(III), and Sb(III)

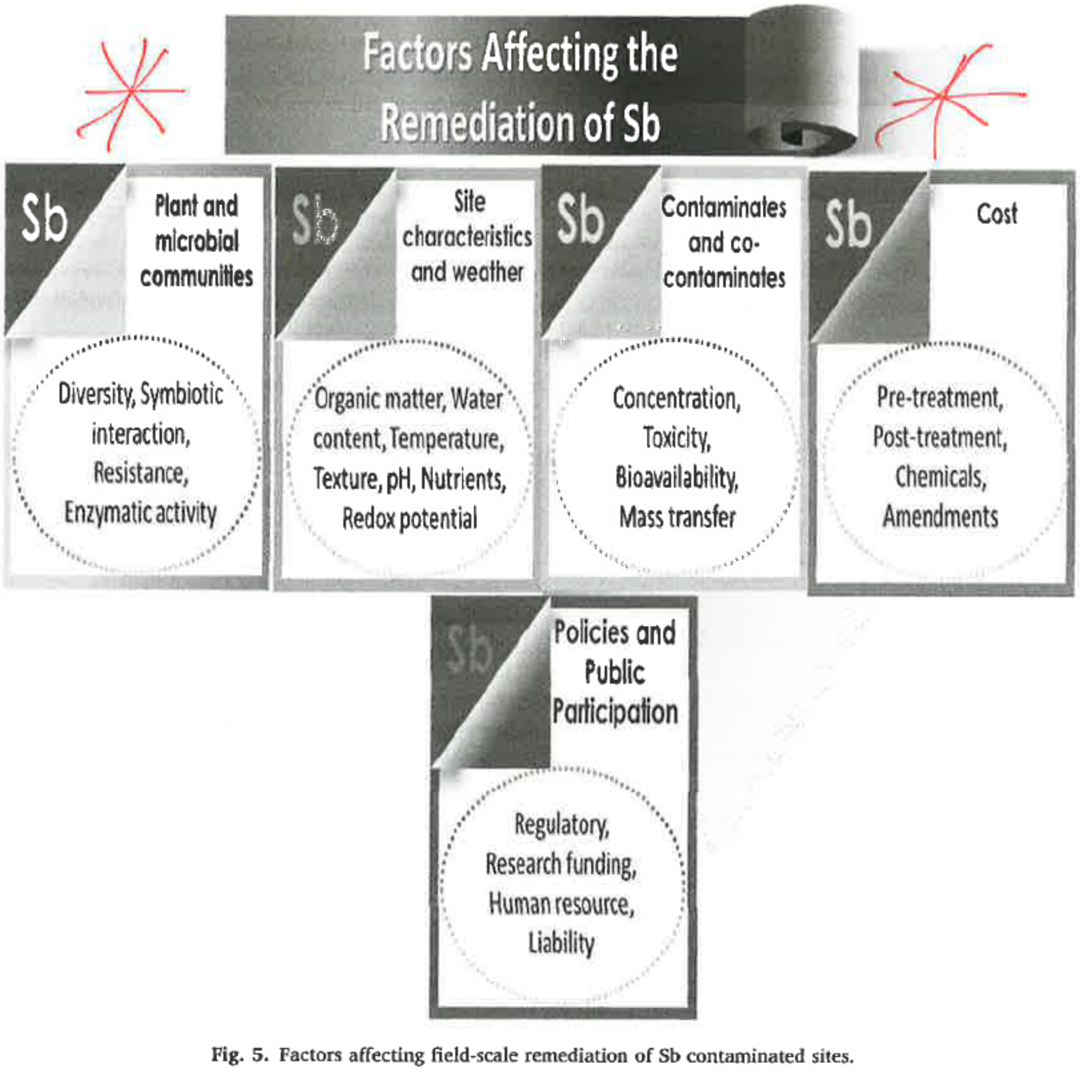

Fig. 5. Factors affecting field-scale remediation of Sb contaminated sites.

became firmly bound with iron oxide/hydroxide over a wide-ranging pH (Almås et al., 2019; Tandy et al., 2017). Biochar modified with Fe-Mn immobilized Sb in a contaminated soil and thereby, reducing Sb phytoavailability in the soil (Wang et al., 2019c). Moreover, the amendment of Fe-modified biochar to agricultural soil increased Sb retention and soil fertility (Wang et al., 2019c). The influence of urea on Sb bioavailability in a paddy-field soil was investigated by Zhang et al. (2021b). The results demonstrated that, at the beginning (15–45 days after treatment), Sb bioavailability extracted by ammonium sulfate increased compared to the control soil (9.5–9.8 vs. 10.1–14 mg kg^{-1}) due to the higher soil pH releasing adsorbed and organic-bound Sb from the soil. After 120 days of experimentation, reduced Sb bioavailability was observed due to the enhanced affinity of Sb toward iron oxides present in the soil. Immobilization of Sb, as shown in various studies, and its efficiencies, are given in Table 3**(a)**. Although the application of such soil amendments results in the high retention of metal(loids), some drawbacks have not been rectified. In addition, any change in soil conditions (e.g., pH) can activate the bioavailability of metal(loids) (Wuana and Okieimen, 2011). Most studies have focused only on one aspect (i.e., Sb immobilization). However, it is important to investigate the associated changes in activities of soil enzymes and fertility.

6.2. *Mobilization using soil leaching*

The mobilization of Sb in contaminated soils has not been carried out to a great extent, mainly due to the high cost of the chelators. Various chelating agents, both organic and inorganic, such as ethylenediaminetetraacetic acid (EDTA), polyacrylic acid, acetic acid, oxalic acid, citrate, ethylenediamine tetra(methylene phosphonic acid), ammonium oxalate, ammonium acetate, calcium chloride, ammonium nitrate, and disodium hydrogen phosphate, have been assessed (Filella, 2011). A low level of Sb was leached from the soil using gentle extractants, and a better-leached yield of Sb was achieved by organic extractants, except EDTA (Filella, 2011). Tan et al. (2018) subjected lightly, moderately, and highly contaminated soils to a leaching process with different extractants; the results showed that the efficiency of extractants in leaching Sb from the soils decreased in the order of citric acid, tartaric acid, EDTA, hydrochloric acid, disodium hydrogen phosphate, and calcium chloride. Interestingly, in a highly Sb contaminated soil (6,876 mg kg^{-1}), water leached up to of 94.8 mg kg^{-1} Sb (Tan et al., 2018). Water and disodium hydrogen phosphate mobilized almost equal amounts of Sb (Soil No. 1: 0.6 mg L^{-1} and Soil No. 2: 0.3 mg L^{-1}) (Cappuyns and Van Campen, 2020). The efficiencies of mobilization data are presented in Table 3**(b)**.

6.3. *Phytoremediation*

Phytoremediation is a lengthy but cost-effective, and aesthetically accepted approach used to remediate environmentally harmful metal (loids)/pollutants including Sb (Antoniadis et al., 2021; Fuke et al., 2021; Kumar et al., 2021c; Mensah et al., 2021; Prabha et al., 2021). It is a greener and environmentally sustainable remediation technique, than other physicochemical methods for metal mobilization and immobilization (Gunarathne et al., 2020). Most data are from laboratory (pot) experiments, in which the soil has been spiked with Sb. However, spiking does not represent the same mineralogical composition of the Sb-derivatives and leads to rapid bioavailability. Müller et al. (2013) conducted a 7-week pot experiment with Sb. A clean soil spiked with 5, 10, and 16 mg kg^{-1} of Sb and an Sb-contaminated soil (14 mg kg^{-1}) from an abandoned mine area were used. The authors also studied the effect of a co-contaminant (arsenic) added at a rate of 20 mg kg^{-1} on the studied plant species (*Pteris vittate*, a fern). A significant amount (232.6 mg kg^{-1}) of Sb was taken up by the plant when grown in the pots spiked with 5 mg kg^{-1} and grown with the co-contaminant, but only 52.9 mg kg^{-1} was taken up when the plants were exposed only to Sb. Sb accumulated in the roots (230 mg kg^{-1}) rather than in the shoots (2.6 mg kg^{-1}). Sb in the plants grown in the contaminated mining soil was 20.1 mg kg^{-1} (Müller et al., 2013). In contrast, for *Sorghum bicolor* (sorghum), the Sb concentration in shoots was about 2-fold higher than that in roots (translocation factor was 2.11) (Zand and Heir, 2020). The translocation factor (TF) is calculated by dividing the Sb concentration in shoots by that in roots. If TF > 1, the plant can be used as a good phytoremediator (Antoniadis et al., 2021). Qi et al. (2011) compiled data from 31 plants belonging to 21 families to determine their phytoremediation potential; they reported Sb concentrations in the plants ranging from 3.92 to 143.69 mg kg^{-1}. The TF values of some plants are displayed in Table 3 **(c)**. A few of the plants, such as *Barbarea verna* (a type of cress), *Sorghum bicolor* (sorghum), and *Nicotiana* (tobacco) (Family: Solanaceae) had TF > 1, and plants might be potential phytoremediators for Sb.

6.4. *Microbial remediation*

Microbial communities in soils are crucial biotic factors in the remediation of potential toxic elements such as Sb, via bio-oxidation and bio-reduction, which change the toxicity, mobility, and labile nature of Sb by altering its chemical properties (He et al., 2019b; Jeyasundar et al., 2021). Numerous Sb-oxidizing bacteria species have been reported. For instance, *Acinetobacter* sp., *Stenotrophomonas* sp., *Comamonas* sp., *Shinella* sp., *Hydrogenophaga* sp., *Variovorax* sp., *Variovorax* sp., and *Flavihumibacter stibioxidans*; these strains facilitate Sb (III) oxidation to Sb (V) under aerobic conditions (Han et al., 2016; He et al., 2019b). One strain of *Shinella* sp. (NLS1) and one strain of *Ensifer* sp. (NLS4), isolated and screened from Sb-polluted soil, showed optimum Sb (III) oxidation in agar media with and without the presence of yeast extract (Choi et al., 2017) (Table 3**(d)**). However, some strains belonging to the order Bacillales (Lai et al., 2016; Lai et al., 2018) transmuted Sb(V) to Sb (III) under anoxic conditions. A new strain belonging to the *Sinorhizobium* genus was isolated from Sb-contaminated sediment; it reduced Sb (V) to Sb (III) in the presence of acetate under anaerobic conditions (Nguyen and Lee, 2014). Another bioremediation process in the microbial community is the methylation of inorganic Sb. Methylated Sb exhibits less toxicity than pentavalent Sb and trivalent Sb (He et al., 2019b). The production of monomethyl Sb, dimethyl Sb, and trimethyl Sb by microbial communities has been well documented (Andrewes et al., 2000; Hartmann et al., 2003). However, no studies have been performed to demonstrate the immobilization of microbially methylated Sb in soil using amendments.

6.5. *Integrated risk management*

An integrated approach incorporates a set of remediation strategies deployed to remediate contaminated environments (Kumar et al., 2021b; Sun et al., 2020). Several researchers (e.g., Chirakkara et al., 2015; Girolkar et al., 2021; Sánchez et al., 2020) have studied this topic. Couto et al. (2015) used phytoremediation, coupled with electrokinetics and a phosphorus amendment to remove Sb from the soil using Indian mustard (*Brassica juncea*) and ryegrass. The addition of a phosphorus amendment increased Sb uptake by ryegrass by 25% and by Indian mustard by 30% than the plants alone. The phosphorus amendment enhanced Sb desorption from the soil due to the ionic repulsion between phosphate ions and Sb, and Sb bioavailability increased with a low-intensity electric field (Couto et al., 2015). Effects of TiO_2 nanoparticles on the phytoremediation of Sb using *Sorghum bicolor* was undertaken by Zand and Heir (2020). The plant was exposed to varying dosages of TiO_2 nanoparticles (from 0 to 1000 mg kg^{-1}). Increased total plant biomass, plant uptake and translocation of Sb in the pots containing 50–250 mg kg^{-1} TiO_2 relative to those in the control soil (without TiO_2) were reported (Zand and Heir, 2020).

7. Summary and future research needs

Environmental Sb contamination is triggered by natural processes

Table 3
The remediation process of antimony (Sb (III) and Sb (V)).

Environmental matrix	Initial concentration	Amendment	Efficiency	References
(a) Immobilization Retention efficiency				
Soil/Slag (50.00 g/50.00 g)	72.7.0 mg kg^{-1}	$FeSO_4$ (4.00 g)	99.25%	Almås et al. (2019)
Soil/Slag (45.00 g/10.00 g)	72.70 mg kg^{-1}	Peat soil (45.00 g)	39.15%	
Soil	79.24 mg kg^{-1}	Fe-Mn biochar (0.5% w/w)	33.80%	Wang et al. (2019c)
		Fe-Mn biochar (1.00% w/w)	40.50%	
		Fe-Mn biochar (2.00% w/w)	43.50%	
Low TOC soil	100.00 mg kg^{-1}	Pristine biochar (20.00% w/w)	12.00%	Silvani et al. (2019)
		Fe-enriched biochar (20.00% w/w)	47.00%	
High TOC soil	210.00 mg kg^{-1}	Pristine biochar (20.00% w/w)v	90.00%	
		Fe-enriched biochar (20.00% w/w)	60.00%	
Soil (4.00 g)	445.165 μg kg^{-1} leached concentration of Sb in unamended	Zero valent Fe^0 (1:19 ratio to soil)	6.66%	Tandy et al. (2017)
		$FeSO_4$ (1:19 ratio to soil)	98.32%	
		Viro-Soil 1 (1:4 ratio to soil)	76.52%, 47.62%	
		Fe^0: Viro-Soil 1: soil (4:19:76)	79.37%	
		Fe^0: Viro-Soil 2: soil (4:19:76)	36.24%	
		$FeSO_4$: Viro-Soil 1: soil (4:19:76)	97.19%	
		$FeSO_4$: Viro-Soil 2: soil (4:19:76)	96.74%	
			Decrease in Sb leaching	
Fly ash	2.04 ± 0.06 mg L^{-1}	Laboratory iron–rich residuals (LIR–1 and LIR–2) (1.75% w/w)	3.53–6.53% and 4.68–10.58% by LIR–1 and LIR–2 respectively	Wang et al. (2019b)
Soil (70.00 g)	Column leached concentration of Sb in unamended: 35.34 μg	Kaolinite 8.00% (w/w)	46.50%	Doherty et al. (2017)
		Kaolinite 10.00% (w/w)	44.70%	
		Zero valent Fe 1.00% (w/w)	67.00%	
		Zero valent Fe 3.00% (w/w)	82.30%	
		Zero valent Fe 5.00% (w/w)	72.30%	
		Ferrihydrite 1.00% (w/w)	82.00%	
		Ferrihydrite 3.00% (w/w)	92.60%	
		Ferrihydrite 5.00% (w/w)	93.30%	
		Ferric chloride 1.00% (w/w)	74.90%	
		Ferric chloride 3.00% (w/w)	54.60%	
(b) Mobilization/leaching process			**Leaching percentage/amount**	
Soil (5.00 g)	1234.70 mg kg^{-1}*	EDTA (25.00 mL, 0.05 M) and few drops of 1.00 M NaOH	Mean: 7.464% (n = 12)	Zhang et al. (2018)
Soil (2.50 g)	1234.70 mg kg^{-1}*	Na_2HPO_4 (25.00 mL, 0.10 M)	Mean: 1.741% (n = 12)	
Soil (2.50 g)	1234.70 mg kg^{-1}*	Ultra-pure H_2O (25.00 mL)	Mean: 0.721% (n = 12)	
Soil 1 and 2 (1.00 g)	Soil 1: 47.00 mg kg^{-1} Soil 2: 95.00 mg kg^{-1}	Demineralized H_2O (10.00 mL)	Soil 1: 0.612 mg L^{-1} Soil 2: 0.284 mg L^{-1}	Cappuyns et al. (2021)
Soil 1 and 2 (1.00 g)	Soil 1: 47.00 mg kg^{-1} Soil 2: 95.00 mg kg^{-1}	Na_2HPO_4 (10.00 mL, 0.10 M)	Soil 1: 0.635 mg L^{-1} Soil 2: 0.326 mg L^{-1}	
Lightly contaminated soil (1.00 g)	145.00 mg kg^{-1}	$CaCl_2$ (20.00 mL, 0.05 M)	0.87 mg kg^{-1}	Tan et al. (2018)
		Na_2HPO_4 (20.00 mL, 0.50 M)	7.39 mg kg^{-1}	
		HCl (20.00 mL, 0.50 M)	7.10 mg kg^{-1}	
		EDTA (20.00 mL, 0.10 M)	8.68 mg kg^{-1}	
		Tartaric acid (20.00 mL, 0.04 M)	21.70 mg kg^{-1}	
		Citric acid (20.00 mL, 0.10 M)	34.40 mg kg^{-1}	
Moderately contaminated soil (1.00 g)	720.00 mg kg^{-1}	$CaCl_2$ (20.00 mL, 0.05 M)	5.32 mg kg^{-1}	
		Na_2HPO_4 (20.00 mL, 0.50 M)	22.20 mg kg^{-1}	
		HCl (20.00 mL, 0.50 M)	17.70 mg kg^{-1}	
		EDTA (20.00 mL, 0.10 M)	57.10 mg kg^{-1}	
		Tartaric acid (20.00 mL, 0.04 M)	64.90 mg kg^{-1}	
		Citric acid (20.00 mL, 0.10 M)	117.00 mg kg^{-1}	
Highly contaminated soil (1.00 g)	6876.00 mg kg^{-1}	$CaCl_2$ (20.00 mL, 0.05 M)	59.40 mg kg^{-1}	
		Na_2HPO_4 (20.00 mL, 0.50 M)	210.00 mg kg^{-1}	
		HCl (20.00 mL, 0.50 M)	478.00 mg kg^{-1}	
		EDTA (20.00 mL, 0.10 M)	1217.00 mg kg^{-1}	
		Tartaric acid (20.00 mL, 0.04 M)	902.00 mg kg^{-1}	
		Citric acid (20.00 mL, 0.10 M)	1449.00 mg kg^{-1}	
Mineral soil (100.00 g)	72.70 mg kg^{-1}	Deionized H_2O (20–30.00 mL)	57.68 mg L^{-1}	Almås et al. (2019)
(c) Phytoremediation		**Plant species**	**Concentration or Translocation factor (TF)**	
Mining area soil	5949.20 mg kg^{-1}	*Hippochcaete ramosissima*	Plant: 98.23 mg kg^{-1}	Qi et al. (2011)
		Rubia leiocaulis	Plant: 66.15 mg kg^{-1}	
		Pteris henryi	Plant: 45.53 mg kg^{-1}	
		Pteris vittate	Plant: 49.16 mg kg^{-1}	
		Debregeasia edulis	Plant: 46.15 mg kg^{-1}	
Mining area soil	2904.00 and 44.40 mg kg^{-1} (aqua regia and EDTA extraction, respectively	*Agrostis capillaris* (Plant collected at mine area)	Root: 402.00 μg g^{-1} Shoot: 69.00 μg g^{-1} TF: 0.172	Bech et al. (2012)
		Agrostis capillaris (Plant potted in a mine soil (20%) and quartz sand (80%) mixture)	Root: 98.75 μg g^{-1} Shoot: 115.68 μg g^{-1} TF: 1.17	

(continued on next page)

Table 3 (*continued*)

Environmental matrix	Initial concentration	Amendment	Efficiency	References
		Agrostis capillaris (Plant potted in a mine soil (50%) and quartz sand (50%) mixture)	Root: 190 $\mu g\ g^{-1}$ Shoot: 45 $\mu g\ g^{-1}$ TF: 0.24	
Mining area soil	152.00 and 19.20 $mg\ kg^{-1}$ (aqua regia and EDTA extraction, respectively)	*Poa annua*	Root: 19.00 $\mu g\ g^{-1}$ Shoot: 4.60 $\mu g\ g^{-1}$ TF: 0.24	Bech et al. (2012)
		Veronica persica	Root: 5.70 $\mu g\ g^{-1}$ Shoot: 1.70 $\mu g\ g^{-1}$ TF: 0.30	
		Sonchus asper	Root: 3.60 $\mu g\ g^{-1}$ Shoot: 2.60 $\mu g\ g^{-1}$ TF: 0.72	
		Barbarea verna	Root: 1.90 $\mu g\ g^{-1}$ Shoot: 3.10 $\mu g\ g^{-1}$ TF: 1.63	
Mining area soil	–	Bubblejaceae *Buddleja*	Shoot: 14.24 $mg\ kg^{-1}$	Levresse et al. (2012)
		Ruscaeae *Dasylinin*	Shoot: 26.59 $mg\ kg^{-1}$	
		Asteraceae *Gymnosperna*	Root: 20.42 $mg\ kg^{-1}$ Shoot: 22.52 $mg\ kg^{-1}$ TF: 1.10	
		Pinaceae *Pinus*	Shoot: 26.63 $mg\ kg^{-1}$	
Soil from waste tailing area	–	Solanaceae *Nicotiana*	Root: 4.72 $mg\ kg^{-1}$ Shoot: 191.32 $mg\ kg^{-1}$ TF: 40.53	Levresse et al. (2012)
		Cupressaceae *Junipesus*	Shoot: 250.64 $mg\ kg^{-1}$	
		Asphodelaceae *Asphodelus*	Root: 447.52 $mg\ kg^{-1}$ Shoot: 29.42 $mg\ kg^{-1}$ TF: 0.07	
		Myrthaceae *Eucalyptus*	Shoot: 71.57 $mg\ kg^{-1}$	
Soil from abandoned mine	14.00 $mg\ kg^{-1}$	*Pteris vittata*	Root: 25.00 $mg\ kg^{-1}$ Shoot: 0.10 $mg\ kg^{-1}$ TF: 0.004	Müller et al. (2013)
Quartz sand spiked Sb	5.00 $mg\ kg^{-1}$	*Pteris vittata*	Root: 49.00 $mg\ kg^{-1}$ Shoot: 3.90 $mg\ kg^{-1}$ TF: 0.08	
Quartz sand spiked Sb	10.00 $mg\ kg^{-1}$	*Pteris vittata*	Root: 68.00 $mg\ kg^{-1}$ Shoot: 3.40 $mg\ kg^{-1}$ TF: 0.05	
Quartz sand spiked Sb	16.00 $mg\ kg^{-1}$	*Pteris vittata*	Root: 63.00 $mg\ kg^{-1}$ Shoot: 9.60 $mg\ kg^{-1}$ TF: 0.15	
Quartz sand spiked Sb and 5.00 $mg\ kg^{-1}$ As (co-contaminant)	5.00 $mg\ kg^{-1}$	*Sorghum bicolor*	Root: 84.00 $mg\ kg^{-1}$ Shoot: 4.40 $mg\ kg^{-1}$ TF: 0.05	
Quartz sand spiked Sb and 10.00 $mg\ kg^{-1}$ As (co-contaminant)	5.00 $mg\ kg^{-1}$	*Sorghum bicolor*	Root: 94.00 $mg\ kg^{-1}$ Shoot: 4.10 $mg\ kg^{-1}$ TF: 0.04	
Quartz sand spiked Sb and 20.00 $mg\ kg^{-1}$ As (co-contaminant)	5.00 $mg\ kg^{-1}$	*Sorghum bicolor*	Root: 230.00 $mg\ kg^{-1}$ Shoot: 2.60 $mg\ kg^{-1}$ TF: 0.01	
Soil contaminated with Sb	5.00 $mg\ kg^{-1}$	*Sorghum bicolor*	Root: 31.78 $mg\ kg^{-1}$ Shoot: 67.06 $mg\ kg^{-1}$ TF: 2.11	Zand and Heir, (2020)
Sb mining soil	–	*Setaria viridis*	Rhizospheric soils: 311 $mg\ kg^{-1}$ Leaves: 7.58 $mg\ kg^{-1}$ Shoots: 4.40 $mg\ kg^{-1}$	Long et al. (2018)
		Leucospermum gracile	Rhizospheric soils: 74.8 $mg\ kg^{-1}$ Leaves: 38.4 $mg\ kg^{-1}$ Shoots: 24.2 $mg\ kg^{-1}$	
		Cornus canadensis	Rhizospheric soils: 50.4 $mg\ kg^{-1}$ Leaves: 23.3 $mg\ kg^{-1}$ Shoots: 61.5 $mg\ kg^{-1}$	
		Alloteuthis subulatus	Rhizospheric soils: 452 $mg\ kg^{-1}$ Leaves: 174 $mg\ kg^{-1}$ Shoots: 222 $mg\ kg^{-1}$	
		A. thunb	Rhizospheric soils: 132 $mg\ kg^{-1}$ Leaves: 22.3 $mg\ kg^{-1}$ Shoots: 37.5 $mg\ kg^{-1}$	
		S. bunge	Rhizospheric soils: 215 $mg\ kg^{-1}$ Leaves: 70.3 $mg\ kg^{-1}$ Shoots: 31.8 $mg\ kg^{-1}$	
		Buddleja nivea	Rhizospheric soils: 105 $mg\ kg^{-1}$ Leaves:(37.2 $mg\ kg^{-1}$ Shoots: 78.71 $mg\ kg^{-1}$	
		H. bipinnatae		

(*continued on next page*)

Table 3 (*continued*)

Environmental matrix	Initial concentration	Amendment	Efficiency	References
			Rhizospheric soils: 316 mg kg^{-1} Leaves: 55 mg kg^{-1} Shoots: 43.3 mg kg^{-1}	
		Eleusine indica	Rhizospheric soils: 53.8 mg kg^{-1} Leaves: 37.7 mg kg^{-1} Shoots: 39.2 mg kg^{-1}	
		Miscanthus sinensis	Rhizospheric soils: 1561 mg kg^{-1} Leaves: 60.2 mg kg^{-1} Shoots: 66.7 mg kg^{-1}	
		A. lavandulaefolia	Rhizospheric soils: 87.1 mg kg^{-1} Leaves: 28.8 mg kg^{-1} Shoots: 68.6 mg kg^{-1}	
(d) Microbial remediation				
Isolation site		**Microbial species**	**Transformation efficiency/ quantity**	
The strains purified from Sb contaminated soil	500.00 μM	*Shinella* sp. (NLS1) and *Ensifer* sp. (NLS4)	Within 1.5 days 500.00 μM of Sb (III) oxidized to Sb (V)	Choi et al. (2017)
	3069.30 mg kg^{-1}	*Sinorhizobium* sp.	>94.00% of Sb (V) reduced to Sb (III)	
Strain isolated from Sb mining area soil at 4 sites	Site 1: 1240.00 mg kg^{-1} Site 2: 1550.00 mg kg^{-1} Site 3: 650.00 mg kg^{-1} Site 4: 90.00 mg kg^{-1}	*Bacillus* sp. *S3*	100.00% of 100.00 μM Sb (III) oxidized to Sb (V) in 2 days	Nguyen and Lee, (2014)
Strain isolated from Sb mining area soil at 4 sites	Site 1: 1240.00 mg kg^{-1}	*Cupriavidus* sp. *S1*	100.00% of 50.00 μM Sb (III) oxidized to Sb (V) in 12 days	Li et al. (2018a)
	Site 2: 1550.00 mg kg^{-1} Site 3: 650.00 mg kg^{-1} Site 4: 90.00 mg kg^{-1}	*Moraxella* sp. *S2*	50.00% of 50.00 μM Sb (III) oxidized to Sb(V) in 14 days	
Microbial consortia enriched with Sb contaminated soil	–	Microbial consortia	Sb(V) (1 mM) was completely reduced within 1 day	Park and Lee, (2019)
Bacterial strains isolated from the Sb contaminated soils by selective enrichment	14000 mg kg^{-1}	*Arthrobacter* sp. *Aminobacter* sp.	Sb(V) oxidized to Sb_2O_3 or SbO_4	Nam et al. (2018)
Indigenous microbial community	1 mM Sb(III)	Microbial consortia (*Paracoccus, Rhizobium, Achromobacter* and *Hydrogenophaga*)	~100% of Sb(III) was oxidized in 36 h	Zhang et al. (2021a)

* Values calculated, TOC: Total Organic Carbon, Viro-Soil: Red mud derivative.

and anthropological actions. Elevated levels of Sb in the environment pose serious risks to ecosystems and human health in terms of potential toxicity and carcinogenicity. The existence and dispersal of elevated Sb levels in different environmental compartments are of particular concern in many countries. Although Sb exists in various oxidative-state compounds in both organic and inorganic forms, it occurs principally as inorganic Sb(III) and Sb(V) species in terrestrial and aquatic ecosystems. Sb(III) compounds are more mobile and bioavailable, and thus, more toxic to human and ecosystem health, than Sb(V) species. Chemical speciation of Sb plays a significant role in determining its biogeochemical behavior involving dissolution, sorption/desorption, bioavailability, toxicity, and accumulation in organisms. Various techniques have been used to remove Sb from the environment or reduce its toxicity, such as Sb immobilization using amendments (e.g., activated carbon, metal oxides, inorganic minerals), mobilization via soil washing and phytoremediation, and microbial remediation (e.g., Sb(III) methylation). As each technique has its limitations, an integrated approach is often used for sustainable remediation outcomes.

The present review identified some key knowledge gaps regarding Sb contamination and risk management, which warrant the following future research:

I. More data regarding Sb distribution and speciation in different environmental media should be collected to establish the global biogeochemical cycle of Sb.

II. There is relatively little information on Sb levels for different chemical species in environmental media, biota (including flora and fauna), dietary sources, and the human system. The threshold at which Sb has an effect needs to be determined. Therefore, more attention should be paid to assess the ecotoxicology of Sb to fully protect ecosystems and human health.

III. Chemical and microbiological interactions of Sb often have been studied independently in different environmental settings under controlled conditions. However, under realistic environmental conditions, the combined effects of the two factors are much more complicated and need more research.

IV. As bioremediation and phytoremediation are increasingly used as green and sustainable techniques for Sb remediation, Sb biosensors needs to be developed to predict remediation outcomes. Future studies regarding biosensors (e.g., Sb(III)-oxidizing bacteria) would shed more light on the remediation efficiency.

V. Field studies with an integrated approach for the remediation of Sb-contaminated terrestrial and aquatic ecosystems also need to be considered.

Declaration of Competing Interest

The authors declare that they have no known competing financial interests or personal relationships that could have appeared to influence the work reported in this paper.

Acknowledgments

We acknowledge support from the Open Access Publication Fund of the University of Wuppertal, *Germany*. Also, Hailong Wang acknowledges the support from the National Key Research and Development Program of China (2020YFC1807704), and the National Natural Science Foundation of China (21876027).

References

Abad-Valle, P., Álvarez-Ayuso, E., Murciego, A., Muñoz-Centeno, L.M., Alonso-Rojo, P., Villar-Alonso, P., 2018. Arsenic distribution in a pasture area impacted by past mining activities. Ecotoxicology and environmental safety 147, 228–237.

Agency for Toxic Substances and Disease Registry, Atlanta, G., 2019. Toxicological Profile for Antimony. https://www.atsdr.cdc.gov/ToxProfiles/tp.asp? (Accessed 23 August 2021).

Ahmad, M., Lee, S.S., Lim, J.E., Lee, S.-E., Cho, J.S., Moon, D.H., Hashimoto, Y., Ok, Y.S., 2014. Speciation and phytoavailability of lead and antimony in a small arms range soil amended with mussel shell, cow bone and biochar: EXAFS spectroscopy and chemical extractions. Chemosphere 95, 433–441.

Alderton, D.H., Serafimovski, T., Burns, L., Tasev, G., 2014. Distribution and mobility of arsenic and antimony at mine sites in FYR Macedonia. Carpathian Journal of Earth and Environmental Sciences 9 (1), 43–56.

Almås, Å.R., Pironin, E., Okkenhaug, G., 2019. The partitioning of Sb in contaminated soils after being immobilization by Fe-based amendments is more dynamic compared to Pb. Applied Geochemistry 108, 104378. https://doi.org/10.1016/j.apgeochem.2019.104378.

Álvarez-Ayuso, E., Otones, V., Murciego, A., García-Sánchez, A., Regina, I.S., 2012. Antimony, arsenic and lead distribution in soils and plants of an agricultural area impacted by former mining activities. Science of the Total Environment 439, 35–43.

Andrewes, P., Cullen, W.R., Polishchuk, E., 2000. Antimony biomethylation by Scopulariopsis brevicaulis: characterization of intermediates and the methyl donor. Chemosphere 41 (11), 1717–1725.

Antoniadis, V., Shaheen, S.M., Stärk, H.-J., Wennrich, R., Levizou, E., Merbach, I., Rinklebe, J., 2021. Phytoremediation potential of twelve wild plant species for toxic elements in a contaminated soil. Environ. Int. 146, 106233. https://doi.org/10.1016/j.envint.2020.106233.

Antoniadis, V., Golia, E.E., Liu, Y.-T., Wang, S.-L., Shaheen, S.M., Rinklebe, J., 2019. Soil and maize contamination by trace elements and associated health risk assessment in the industrial area of Volos, Greece. Environment international 124, 79–88.

Armiento, G., Nardi, E., Lucci, F., De Cassan, M., Della Ventura, G., Santini, C., Petrini, E., *Cremisini, C., 2017. Antimony and arsenic distribution in a catchment affected by* past mining activities: influence of extreme weather events. RendicontiLincei 28 (2), 303–315.

Artzer, A., Moats, M., Bender, J., 2018. Removal of antimony and bismuth from copper electrorefining electrolyte: Part I—a review. Jom 70 (10), 2033–2040.

Asaoka, S., Takahashi, Y., Araki, Y., Tanimizu, M., 2012. Comparison of antimony and arsenic behavior in an Ichinokawa River water–sediment system. Chemical Geology 334, 1–8.

Ashley, P.M., Graham, B.P., Tighe, M.K., Wolfenden, B.J., 2007. Antimony and arsenic dispersion in the Macleay River catchment, New South Wales: a study of the environmental geochemical consequences. Australian Journal of Earth Sciences 54 (1), 83–103.

Baek, Y.-W., Lee, W.-M., Jeong, S.-W., An, Y.-J., 2014. Ecological effects of soil antimony on the crop plant growth and earthworm activity. Environmental earth sciences 71 (2), 895–900.

Baeza, M., Ren, J., Krishnamurthy, S., Vaughan, T.C., 2010. Spatial distribution of antimony and arsenic levels in Manadas Creek, an urban tributary of the Rio Grande in Laredo, Texas. Archives of environmental contamination and toxicology 58 (2), 299–314.

Bagherifam, S., Brown, T.C., Fellows, C.M., Naidu, R., 2019a. Bioavailability of arsenic and antimony in terrestrial ecosystems: a review. Pedosphere 29 (6), 681–720.

Bagherifam, S., Brown, T.C., Fellows, C.M., Naidu, R., 2019b. Derivation methods of soils, water and sediments toxicity guidelines: A brief review with a focus on antimony. Journal of Geochemical Exploration 205, 106348. https://doi.org/10.1016/j.gexplo.2019.106348.

Bech, J., Corrales, I., Tume, P., Barceló, J., Duran, P., Roca, N., Poschenrieder, C., 2012. Accumulation of antimony and other potentially toxic elements in plants around a former antimony mine located in the Ribes Valley (Eastern Pyrenees). Journal of Geochemical Exploration 113, 100–105.

Belzile, N., Chen, Y.-W., Wang, Z., 2001. Oxidation of antimony (III) by amorphous iron and manganese oxyhydroxides. Chemical Geology 174 (4), 379–387.

Bergmann, M.E.H., Koparal, A.S., 2007. Kinetic studies on electrochemical antimony removal from concentrated sulfuric acid systems. Chemical Engineering & Technology: Industrial Chemistry-Plant Equipment-Process Engineering-Biotechnology 30 (2), 242–249.

Bolan, N., Hoang, S.A., Beiyuan, J., Gupta, S., Hou, D., Karakoti, A., Joseph, S., Jung, S., Kim, K.H., Kirkham, M.B. and Kua, H.W., 2021. Multifunctional applications of biochar beyond carbon storage. International Materials Reviews, pp.1-51. https://doi.org/10.1080/09506608.2021.1922047.

Bolan, N.S., Ko, B.G., Anderson, C.W.N., Vogeler, I., Mahimairaja, S., Naidu, R., 2008. Manipulating bioavailability to manage remediation of metal-contaminated soils. Developments in soil science 32, 657–678.

Buschmann, J., Sigg, L., 2004. Antimony (III) binding to humic substances: influence of pH and type of humic acid. Environmental science & technology 38 (17), 4535–4541.

Campos, T., Chaer, G., Leles, P.D.S., Silva, M., Santos, F., 2019. Leaching of heavy metals in soils conditioned with biosolids from sewage sludge. Floresta e Ambiente 26 (SPE1).

Cappuyns, V. and Van Campen, A., 2020. Antimony in soils and mine waste heaps around the Mau Due antimony mine, North-Vietnam. In International Conference on Heavy Metals in the Environment (ICHMET), Date: 2020/10/25-2020/10/29, Location: Seoul, South Korea/Virtual (pp. 137-137).

Cappuyns, V., Van Campen, A., Helser, J., 2021. Antimony leaching from soils and mine waste from the Mau Due antimony mine. North-Vietnam. Journal of Geochemical Exploration 220, 106663. https://doi.org/10.1016/j.gexplo.2020.106663.

Chang, A.C., Pan, G., Page, A.L., Asano, T., 2002. Developing Human Health-related Chemical Guidelines for Reclaimed Wastewater and Sewage Sludge Applications in Agriculture. World Health Organization, Geneva.

Chirakkara, R.A., Reddy, K.R., Cameselle, C., 2015. Electrokinetic amendment in phytoremediation of mixed contaminated soil. Electrochimica Acta 181, 179–191.

Choi, W., Yu, J., Lee, T., 2017. Microbial oxidation of antimonite and arsenite by bacteria isolated from antimony-contaminated soils. International Journal of Hydrogen Energy 42 (45), 27832–27842.

Chu, J., Hu, X., Kong, L., Wang, N., Zhang, S., He, M., Ouyang, W., Liu, X., Lin, C., 2021. Dynamic flow and pollution of antimony from polyethylene terephthalate (PET) fibers in China. Science of The Total Environment 771, 144643. https://doi.org/10.1016/j.scitotenv.2020.144643.

Cidu, R., Biddau, R., Dore, E., Vacca, A., Marini, L., 2014. "Antimony in the soil–water–plant system at the Su Suergiu abandoned mine (Sardinia, Italy): Strategies to mitigate contamination.. Science of The Total Environment Volumes 497–498, 319–331.

Conesa, H.M., Wieser, M., Studer, B., Schulin, R., 2011. Effects of vegetation and fertilizer on metal and Sb plant uptake in a calcareous shooting range soil. Ecological Engineering 37 (4), 654–658.

Constantino, L.V., Quirino, J.N., Abrão, T., Parreira, P.S., Urbano, A., Santos, M.J., 2018. Sorption–desorption of antimony species onto calcined hydrotalcite: Surface structure and control of competitive anions. Journal of hazardous materials 344, 649–656.

Corrales, I., Barceló, J., Bech, J., Poschenrieder, C., 2014. Antimony accumulation and toxicity tolerance mechanisms in Trifolium species. Journal of Geochemical Exploration 147, 167–172.

Coughlin, O., Krämer, T., Benjamin, S.L., 2020. Diverse structure and reactivity of pentamethylcyclopentadienyl antimony (iii) cations. Dalton Transactions 49 (6), 1726–1730.

Council of the European Union, 1998. Council Directive 98/83/EC of 3 November 1998 on the quality of water intended for human consumption. Off J Eur Communities [Internet], 41, pp.34-54.

Couto, N., Guedes, P., Zhou, D.-M., Ribeiro, A.B., 2015. Integrated perspectives of a greenhouse study to upgrade an antimony and arsenic mine soil–Potential of enhanced phytotechnologies. Chemical Engineering Journal 262, 563–570.

Cullen, A., Kiberd, B., Devaney, D., Gillan, J., Kelehan, P., Matthews, T.G., Mayne, P., Murphy, N., O'Regan, M., Shannon, W., Thornton, L., 2000. Concentrations of antimony in infants dying from SIDS and infants dying from other causes. Archives of disease in childhood 82 (3), 244–247.

Denys, S., Caboche, J., Tack, K., Rychen, G., Wragg, J., Cave, M., Jondreville, C., Feidt, C., 2012. In vivo validation of the unified BARGE method to assess the *bioaccessibility of arsenic, antimony, cadmium, and lead in soils. Environmental* science & technology 46 (11), 6252–6260.

Diquattro, S., Castaldi, P., Ritch, S., Juhasz, A.L., Brunetti, G., Scheckel, K.G., Garau, G., Lombi, E., 2021. Insights into the fate of antimony (Sb) in contaminated soils: Ageing influence on Sb mobility, bioavailability, bioaccessibility and speciation. Science of The Total Environment 770, 145354. https://doi.org/10.1016/j.scitotenv.2021.145354.

Diquattro, S., Garau, G., Mangia, N.P., Drigo, B., Lombi, E., Vasileiadis, S., Castaldi, P., 2020. Mobility and potential bioavailability of antimony in contaminated soils: Short-term impact on microbial community and soil biochemical functioning. Ecotoxicology and environmental safety 196, 110576. https://doi.org/10.1016/j.ecoenv.2020.110576.

Doherty, S.J., Tighe, M.K., Wilson, S.C., 2017. Evaluation of amendments to reduce arsenic and antimony leaching from co-contaminated soils. Chemosphere 174, 208–217.

Dousova, B., Buzek, F., Herzogova, L., Machovic, V., Lhotka, M., 2015. Effect of organic matter on arsenic(V) and antimony(V) adsorption in soils. Eur. J. Soil Sci. 66 (1), 74–82.

Dupont, D., Arnout, S., Jones, P.T., Binnemans, K., 2016. Antimony recovery from end-of-life products and industrial process residues: a critical review. Journal of Sustainable Metallurgy 2 (1), 79–103.

Elbaz-Poulichet, F., Guédron, S., Anne-Lise, D., Freydier, R., Perrot, V., Rossi, M., Piot, C., Delpoux, S., Sabatier, P., 2020. "A 10,000-year record of trace metal and metalloid (Cu, Hg, Sb, Pb) deposition in a western Alpine lake (Lake Robert, France): Deciphering local and regional mining contamination". Quaternary Science Reviews Volume 228 (ISSN 106076). 0277–3791.

Elleouet, C., Quentel, F., Madec, C.L., Fileila, M., 2005. The effect of the presence of trace metals on the oxidation of Sb (III) by hydrogen peroxide in aqueous solution. Journal of Environmental Monitoring 7 (12), 1220–1225.

El-Naggar, A., Shaheen, S.M., Hseu, Z.-Y., Wang, S.-L., Ok, Y.S., Rinklebe, J., 2019. Release dynamics of As Co, and Mo in a biochar treated soil under pre-definite redox conditions. Science of the Total Environment 657, 686–695.

El-Naggar, A., Shaheen, S.M., Ok, Y.S., Rinklebe, J., 2018. Biochar affects the dissolved and colloidal concentrations of Cd, Cu, Ni, and Zn and their phytoavailability and potential mobility in a mining soil under dynamic redox-conditions. Science of the total environment 624, 1059–1071.

Etim, E.U., 2017. Occurrence and distribution of arsenic, antimony and selenium in shallow groundwater systems of Ibadan Metropolis, Southwestern Nigerian. Journal of Health and Pollution 7 (13), 32–41.

Ettler, V., Mihaljevič, M., Šebek, O., Nechutný, Z., 2007. Antimony availability in highly polluted soils and sediments - A comparison of single extractions. Chemosphere 68 (3), 455–463.

Ettler, V., Tejnecký, V., Mihaljevic, M., Sebek, O., Zuna, M., Vanek, A., 2010. Antimony mobility in lead smelter-polluted soils. Geoderma 155 (3-4), 409–418.

Fan, Y., Zheng, C., Liu, H., He, C., Shen, Z., Zhang, T.C., 2020. Effect of pH on the adsorption of arsenic (V) and antimony (V) by the black soil in three systems: Performance and mechanism. Ecotoxicology and environmental safety 191, 110145. https://doi.org/10.1016/j.ecoenv.2019.110145.

Feng, RenWei, Lei, L., Su, JunMing, Zhang, RuiRui, Zhu, YanMing, Chen, WenXiang, Wang, LiZhen, Wang, RenJie, Dai, JiaXin, Lin, ZiTing, Li, YuanPing, Liu, BiXiu, Fan, ZhiLian, Liu, H., Rensing, C., 2020. Toxicity of different forms of antimony to rice plant: Effects on root exudates, cell wall components, endogenous hormones and antioxidant system. Science of The Total Environment 711, 134589. https://doi.org/10.1016/j.scitotenv.2019.134589.

Feng, R., Liao, G., Guo, J., Wang, R., Xu, Y., Ding, Y., Mo, L., Fan, Z., Li, N., 2016. Responses of root growth and antioxidative systems of paddy rice exposed to antimony and selenium. Environmental and Experimental Botany 122, 29–38.

Feng, R., Wei, C., Tu, S., Ding, Y., Wang, R., Guo, J., 2013. The uptake and detoxification of antimony by plants: a review. Environmental and experimental botany 96, 28–34.

Filella, M., May, P.M., 2003. Computer simulation of the low-molecular-weight inorganic species distribution of antimony (III) and antimony (V) in natural waters. Geochimica et Cosmochimica Acta 67 (21), 4013–4031.

Filella, M., May, P.M., 2005. Critical appraisal of available thermodynamic data for the complexation of antimony (III) and antimony (V) by low molecular mass organic ligands. Journal of Environmental Monitoring 7 (12), 1226–1237.

Filella, M., Williams, P.A., 2012. Antimony interactions with heterogeneous complexants in waters, sediments and soils: a review of binding data for homologous compounds. Geochemistry 72, 49–65.

Filella, M., 2011. Antimony interactions with heterogeneous complexants in waters, sediments and soils: a review of data obtained in bulk samples. Earth-Science Reviews 107 (3-4), 325–341.

Filella, M., Belzile, N., Chen, Y.-W., 2002. Antimony in the environment: a review focused on natural waters: I. Occurrence. Earth-Science Reviews 57 (1-2), 125–176.

Filella, M., Belzile, N., Lett, M.C., 2007. Antimony in the environment: a review focused on natural waters. III. Microbiota relevant interactions. Earth-Science Reviews 80 (3–4), 195–217.

Filella, M., Hennebert, P., Okkenhaug, G., Turner, A., 2020. Occurrence and fate of antimony in plastics. Journal of hazardous materials 390, 121764.

Flynn, H.C., Meharg, A.A., Bowyer, P.K., Paton, G.I., 2003. Antimony bioavailability in mine soils. Environmental Pollution 124 (1), 93–100.

Földi, C., Sauermann, S., Dohrmann, R., Mansfeldt, T., 2018. Traffic-related distribution of antimony in roadside soils. Environmental Pollution 237, 704–712.

Fort, M., Grimalt, J.O., Querol, X., Casas, M., Sunyer, J., 2016. Evaluation of atmospheric inputs as possible sources of antimony in pregnant women from urban areas. Science of the Total Environment 544, 391–399.

Frohne, T., Rinklebe, J., Diaz-Bone, R.A., Du Laing, G., 2011. Controlled Variation of Redox Conditions in a Floodplain Soil: Impact on Metal Mobilization and Biomethylation of Arsenic and Antimony. Geoderma 160 (3–4), 414–424.

Fu, Z., Wu, F., Amarasiriwardena, D., Mo, C., Liu, B., Zhu, J., Deng, Q., Liao, H., 2010. Antimony, arsenic and mercury in the aquatic environment and fish in a large antimony mining area in Hunan. China. Science of the Total Environment 408 (16), 3403–3410.

Fu, Z., Wu, F., Mo, C., Deng, Q., Meng, W., Giesy, J.P., 2016. Comparison of arsenic and antimony biogeochemical behavior in water, soil and tailings from Xikuangshan, China. Science of the Total Environment 539, 97–104.

Fuke, P., Kumar, M., Sawarkar, A.D., Pandey, A., Singh, L., 2021. Role of microbial diversity to influence the growth and environmental remediation capacity of bamboo: A review. Industrial Crops and Products 167, 113567.

Gal, J., Hursthouse, A., Cuthbert, S., 2007. Bioavailability of arsenic and antimony in soils from an abandoned mining area, Glendinning (SW Scotland). Journal of Environmental Science and Health Part A 42 (9), 1263–1274.

Gallagher, M.J., Stone, P., Kemp, A.E.S., Hills, M.G., Jones, R.C., Smith, R.T., Peachey, D., Vickers, B.P., Parker, M.E., Rollin, K.E. and Skilton, B.R.H., 1983. Stratabound arsenic and vein antimony mineralisation in Silurian greywackes at Glendinning, South Scotland.

Geng, L., Yang, Z., Xu, Z., 2020. Effects of antimony contamination in soil on the nutrient composition of three green leafy vegetables. Journal of Soils and Sediments 20, 2217–2224.

Girolkar, S., Thawale, P. and Juwarkar, A., 2021. Bacteria-assisted phytoremediation of heavy metals and organic pollutants: challenges and future prospects. In Bioremediation for Environmental Sustainability (pp. 247-267). Elsevier.

Greenberg, M.S., Schoeters, I., Wentsel, R.S., Charters, D.W., Mitchell, I.A., Zajdlik, B., 2014. Regulatory considerations for the potential development and application of metal cleanup values. Integrated environmental assessment and management 10 (3), 401–414.

Grob, M., Wilcke, W., Mestrot, A., 2018. Release and biomethylation of antimony in shooting range soils upon flooding. Soil systems 2 (2), 34.

Groth, D.H., Stettler, L.E., Burg, J.R., Busey, W.M., Grant, G.C., Wong, L., 1986. Carcinogenic effects of antimony trioxide and antimony ore concentrate in rats. Journal of Toxicology and Environmental Health, Part A Current Issues 18 (4), 607–626.

Gunarathne, V., Gunatilake, S.R., Wanasinghe, S.T., Atugoda, T., Wijekoon, P., Biswas, J. K., Vithanage, M., 2020. Phytoremediation for E-waste contaminated sites. In: Handbook of Electronic Waste Management. Butterworth-Heinemann, pp. 141–170.

Guo, Q., Planer-Friedrich, B., Luo, L., Liu, M., Wu, G., Li, Y., Zhao, Q., 2020. Speciation of antimony in representative sulfidic hot springs in the YST Geothermal Province (China) and its immobilization by spring sediments. Environmental Pollution 266, 115221.

Guo, W., Fu, Z., Wang, H., Song, F., Wu, F., Giesy, J.P., 2018. Environmental geochemical and spatial/temporal behavior of total and speciation of antimony in typical contaminated aquatic environment from Xikuangshan, China. Microchemical Journal 137, 181–189.

Guo, X., Wu, Z., He, M., 2009. Removal of antimony (V) and antimony (III) from drinking water by coagulation- flocculation -sedimentation (CFS). Water research 43 (17), 4327–4335.

Han, Y., Zhang, F., Wang, Q., Zheng, S., Guo, W., Feng, L., Wang, G., 2016. Flavihumibacter stibioxidans sp. nov., an antimony-oxidizing bacterium isolated from antimony mine soil. International journal of systematic and evolutionary microbiology 66 (11), 4676–4680.

Hartmann, L.M., Craig, P.J., Jenkins, R.O., 2003. Influence of arsenic on antimony methylation by the aerobic yeast Cryptococcus humicolus. Archives of microbiology 180 (5), 347–352.

He, M., 2007. Distribution and phytoavailability of antimony at an antimony mining and smelting area, Hunan, China. Environmental Geochemistry and Health 29 (3), 209–219.

He, M., Wang, N., Long, X., Zhang, C., Ma, C., Zhong, Q., Wang, A., Wang, Y., Pervaiz, A., Shan, J., 2019a. Antimony speciation in the environment: Recent advances in understanding the biogeochemical processes and ecological effects. Journal of Environmental Sciences 75, 14–39.

He, M., Wang, X., Wu, F., Fu, Z., 2012. Antimony pollution in China. Science of the total environment 421, 41–50.

He, Z., Wei, Z., Zhang, Q., Zou, J., Pan, X., 2019b. Metal oxyanion removal from wastewater using manganese-oxidizing aerobic granular sludge. Chemosphere 236, 124353.

Herath, I., Vithanage, M., Bundschuh, J., 2017. Antimony as a global dilemma: geochemistry, mobility, fate and transport. Environmental pollution 223, 545–559.

Hiller, E., Lalinská, B., Chovan, M., Jurkovič, Ľ., Klimko, T., Jankulár, M., Hovorič, R., Šottník, P., Fľaková, R., Zenišová, Z., Ondrejková, I., 2012. Arsenic and antimony contamination of waters, stream sediments and soils in the vicinity of abandoned antimony mines in the Western Carpathians, Slovakia. Applied Geochemistry 27 (3), 598–614.

Hu, L., Fu, J., Wang, S., Xiang, Y., Pan, X., 2021. Microplastics generated under simulated fire scenarios: Characteristics, antimony leaching, and toxicity. Environmental Pollution 269, 115905.

Hua, J., Wu, C., Zhang, H., Cao, L., Wei, T., Guo, J., 2021. Biochar-induced changes in soil microbial affect species of antimony in contaminated soils. Chemosphere 263, 127795.

Huang, T., Liu, L., Xu, J., Zhang, S., 2019. Combination of electrokinetics and nano zero-valent iron-based adsorption enhances Sb (V) removal from feed water in the batch and column mode processes. Desalination and Water Treatment 150, 166–191.

Huang, Y., Chen, Z., Liu, W., 2012. Influence of iron plaque and cultivars on antimony uptake by and translocation in rice (Oryza sativa L.) seedlings exposed to Sb (III) or Sb (V). Plant and Soil 352 (1), 41–49.

IARC, 1989. Antimony trioxide and antimony trisulfide. Some Organic Solvents, Resin Monomers and Related Compounds, Pigments and Occupational Exposures in Paint Manufacture and Painting Vol. 47. IARC Monographs on the Evaluation of Carcinogenic Risks to Humans, pp. 291–305.

Iijima, A., Sato, K., Yano, K., Kato, M., Kozawa, K., Furuta, N., 2008. Emission factor for antimony in brake abrasion dusts as one of the major atmospheric antimony sources. Environmental science & technology 42 (8), 2937–2942.

Inam, M.A., Khan, R., Park, D.R., Khan, S., Uddin, A., Yeom, I.T., 2019. Complexation of antimony with natural organic matter: Performance evaluation during coagulation-flocculation process. International journal of environmental research and public health 16 (7), 1092.

Intrakamhaeng, V., Clavier, K.A., Liu, Y., Townsend, T.G., 2020. Antimony mobility from E-waste plastic in simulated municipal solid waste landfills. Chemosphere 241, 125042.

Jabłońska-Czapla, M., Szopa, S., Zerzucha, P., Łyko, A., Michalski, R., 2015. Chemometric and environmental assessment of arsenic, antimony, and chromium speciation form occurrence in a water reservoir subjected to thermal anthropopressure. Environmental Science and Pollution Research 22 (20), 15731–15744.

James, E., Turner, A., 2020. Mobilisation of antimony from microplastics added to coastal sediment. Environmental Pollution 264, 114696.

Jenkins, R.O., Morris, T.A., Craig, P.J., Goessler, W., Ostah, N., Wills, K.M., 2000. Evaluation of cot mattress inner foam as a potential site for microbial generation of toxic gases. Human & experimental toxicology 19 (12), 693–702.

Jeyasundar, P.G.S.A., Ali, A., Azeem, M., Li, Y., Guo, D., Sikdar, A., Abdelrahman, H., Kwon, E., Antoniadis, V., Mani, V.M., Shaheen, S.M., 2021. Green remediation of toxic metals contaminated mining soil using bacterial consortium and Brassica juncea. Environmental Pollution 277, 116789.

Ji, Y., Sarret, G., Schulin, R., Tandy, S., 2017. Fate and chemical speciation of antimony (Sb) during uptake, translocation and storage by rye grass using XANES spectroscopy. Environmental Pollution 231, 1322–1329.

Jia, X., Zhou, J., Liu, J., Liu, P., Yu, L., Wen, B., Feng, Y., 2020. The antimony sorption and transport mechanisms in removal experiment by Mn-coated biochar. Science of The Total Environment 724, 138158.

Johnson, C.A., Moench, H., Wersin, P., Kugler, P., Wenger, C., 2005. Solubility of antimony and other elements in samples taken from shooting ranges. Journal of environmental quality 34 (1), 248–254.

Kabata-Pendias, A., 2011. Trace elements in soils and plants/fourth editions. CRC Taylor and Francis Group, Boca Raton, p. 505.

Kataoka, T., Mitsunobu, S., Hamamura, N., 2018. Influence of the chemical form of antimony on soil microbial community structure and arsenite oxidation activity. Microbes and environments.

Kosmulski, M., 2009. Compilation of PZC and IEP of sparingly soluble metal oxides and hydroxides from literature. Advances in colloid and interface science 152 (1–2), 14–25.

Kulp, T.R., Miller, L.G., Braiotta, F., Webb, S.M., Kocar, B.D., Blum, J.S., Oremland, R.S., 2014. Microbiological reduction of Sb (V) in anoxic freshwater sediments. Environmental science & technology 48 (1), 218–226.

Kumar, M., Bolan, N.S., Hoang, S.A., Sawarkar, A.D., Jasemizad, T., Gao, B., Keerthanan, S., Padhye, L.P., Singh, L., Kumar, S., Vithanage, M., 2021a. Remediation of soils and sediments polluted with polycyclic aromatic hydrocarbons: To immobilize, mobilize, or degrade? Journal of Hazardous Materials 420, 126534.

Kumar, M., Chen, H., Sarsaiya, S., Qin, S., Liu, H., Awasthi, M.K., Kumar, S., Singh, L., Zhang, Z., Bolan, N.S., Pandey, A., 2020a. Current research trends on micro-and nano-plastics as an emerging threat to global environment: A review. Journal of Hazardous Materials. 124967.

Kumar, M., Dutta, S., You, S., Luo, G., Zhang, S., Show, P.L., Sawarkar, A.D., Singh, L., Tsang, D.C., 2021b. A critical review on biochar for enhancing biogas production from anaerobic digestion of food waste and sludge. Journal of Cleaner Production, 127143.

Kumar, M., Xiong, X., He, M., Tsang, D.C., Gupta, J., Khan, E., Harrad, S., Hou, D., Ok, Y. S., Bolan, N.S., 2020b. Microplastics as pollutants in agricultural soils. Environmental Pollution, 114980.

Kumar, M., Xiong, X., Sun, Y., Yu, I.K., Tsang, D.C., Hou, D., Gupta, J., Bhaskar, T., Pandey, A., 2020c. Critical review on biochar-supported catalysts for pollutant degradation and sustainable biorefinery. Advanced Sustainable Systems 4 (10), 1900149.

Kumar, V., Singh, K., Shah, M.P. and Kumar, M., 2021c. Phytocapping: An eco-sustainable green technology for environmental pollution control. In Bioremediation for Environmental Sustainability (pp. 481-491). Elsevier. https://doi.org/10.1016/B978-0-12-820318-7.00022-8.

Kuppusamy, S., Venkateswarlu, K., Megharaj, M., Mayilswami, S., Lee, Y.B., 2017. Risk-based remediation of polluted sites: A critical perspective. Chemosphere 186, 607–615.

Lahermo, P., Tarvainen, T., Hatakka, T., Backman, B., Juntunen, R., Kortelainen, N., Lakomaa, T., Nikkarinen, M., Vesterbacka, P., Väisänen, U., Suomela, P., 2002. One thousand wells–the physical-chemical quality of Finnish well Waters in 1999. Report of investigation 155, 1–92.

Lai, C.Y., Dong, Q.Y., Rittmann, B.E., Zhao, H.P., 2018. Bioreduction of antimonate by anaerobic methane oxidation in a membrane biofilm batch reactor. Environmental science & technology 52 (15), 8693–8700.

Lai, C.Y., Wen, L.L., Zhang, Y., Luo, S.S., Wang, Q.Y., Luo, Y.H., Chen, R., Yang, X., Rittmann, B.E., Zhao, H.P., 2016. Autotrophic antimonate bio-reduction using hydrogen as the electron donor. Water research 88, 467–474.

Lapo, B., Demey, H., Carchi, T., Sastre, A.M., 2019. Antimony removal from water by a chitosan-Iron (III)[ChiFer (III)] biocomposite. Polymers 11 (2), 351.

Laporte-Saumure, M., Martel, R., Mercier, G., 2011. Characterization and metal availability of copper, lead, antimony and zinc contamination at four Canadian small arms firing ranges. Environmental technology 32 (7), 767–781.

Lehr, C.R., Kashyap, D.R., McDermott, T.R., 2007. New insights into microbial oxidation of antimony and arsenic. Applied and environmental microbiology 73 (7), 2386–2389.

Leuz, A.K., Hug, S.J., Wehrli, B., Johnson, C.A., 2006. Iron-mediated oxidation of antimony (III) by oxygen and hydrogen peroxide compared to arsenic (III) oxidation. Environmental science & technology 40 (8), 2565–2571.

Levresse, G., Lopez, G., Tritlla, J., López, E.C., Chavez, A.C., Salvador, E.M., Soler, A., Corbella, M., Sandoval, L.H., Corona-Esquivel, R., 2012. Phytoavailability of antimony and heavy metals in arid regions: the case of the Wadley Sb district (San Luis, Potosí, Mexico). Science of the total environment 427, 115–125.

Lewińska, K., Karczewska, A., 2019. Antimony in soils of SW Poland—an overview of potentially enriched sites. Environmental monitoring and assessment 191 (2), 70.

Lewińska, K., Karczewska, A., Siepak, M., Gałka, B., 2018. The release of antimony from mine dump soils in the presence and absence of forest litter. International journal of environmental research and public health 15 (12), 2631.

Li, J., Wang, Q., Oremland, R.S., Kulp, T.R., Rensing, C., Wang, G., 2016. Microbial antimony biogeochemistry: enzymes, regulation, and related metabolic pathways. Applied and environmental microbiology 82 (18), 5482–5495.

Li, J., Wang, Q., Zhang, S., Qin, D., Wang, G., 2013. Phylogenetic and genome analyses of antimony-oxidizing bacteria isolated from antimony mined soil. International Biodeterioration & Biodegradation 76, 76–80.

Li, J., Wei, Y., Zhao, L., Zhang, J., Shangguan, Y., Li, F., Hou, H., 2014. Bioaccessibility of antimony and arsenic in highly polluted soils of the mine area and health risk assessment associated with oral ingestion exposure. Ecotoxicology and Environmental Safety 110, 308–315.

Li, J., Yu, H., Wu, X., Shen, L., Liu, Y., Qiu, G., Zeng, W., Yu, R., 2018a. Novel hyper antimony-oxidizing bacteria isolated from contaminated mine soils in China. Geomicrobiology journal 35 (8), 713–720.

Li, J., Zhang, Y., Zheng, S., Liu, F., Wang, G., 2019. Anaerobic bacterial immobilization and removal of toxic Sb (III) coupled with Fe (II)/Sb (III) oxidation and denitrification. Frontiers in microbiology 10, 360.

Li, J., Zheng, B., He, Y., Zhou, Y., Chen, X., Ruan, S., Yang, Y., Dai, C., Tang, L., 2018b. Antimony contamination, consequences and removal techniques: A review. Ecotoxicology and Environmental Safety 156, 125–134.

Li, Y., Zhang, M., Xu, R., Lin, H., Sun, X., Xu, F., Gao, P., Kong, T., Xiao, E., Yang, N., Sun, W., 2021. Arsenic and antimony co-contamination influences on soil microbial community composition and functions: Relevance to arsenic resistance and carbon, nitrogen, and sulfur cycling. Environment International 153, 106522.

Lintschinger, J., Koch, I., Serves, S., Feldmann, J., Cullen, W.R., 1997. Determination of antimony species with high-performance liquid chromatography using element specific detection. Fresenius' journal of analytical chemistry 359 (6), 484–491.

Liu, C.Z., Liu, F.L., Xie, Z.B., 2007. LIANG hua-zheng. HUANG De-juan (Faculty of Biology, Chemistry and Material Science, East China Institute of Technology, Fuzhou, JX 344000, China); The Speciation and Bioavailability of Antimony in the Soil near Antimony Mine Area of DeAn [J]. Journal of East China Institute of Technology 4.

Liu, F., Le, X.C., McKnight-Whitford, A., Xia, Y., Wu, F., Elswick, E., Johnson, C.C., Zhu, C., 2010. Antimony speciation and contamination of waters in the Xikuangshan antimony mining and smelting area. China. Environmental geochemistry and health 32 (5), 401–413.

Liu, R., Xu, W., He, Z., Lan, H., Liu, H., Qu, J., Prasai, T., 2015. Adsorption of antimony (V) onto Mn (II)-enriched surfaces of manganese-oxide and FeMn binary oxide. Chemosphere 138, 616–624.

Long, J., Tan, D., Deng, S., Lei, M., 2018. Uptake and accumulation of potentially toxic elements in colonized plant species around the world's largest antimony mine area. China. Environmental geochemistry and health 40 (6), 2383–2394.

Long, J., Zhou, D., Li, B., Zhou, Y., Li, Y., Lei, M., 2020a. The effect of an antimony resistant bacterium on the iron plaque fraction and antimony uptake by rice seedlings. Environmental Pollution 258, 113670.

Long, X., Wang, X., Guo, X., He, M., 2020b. A review of removal technology for antimony in aqueous solution. Journal of Environmental Sciences 90, 189–204.

Loni, P.C., Wu, M., Wang, W., Wang, H., Ma, L., Liu, C., Song, Y., Tuovinen, O.H., 2020. Mechanism of microbial dissolution and oxidation of antimony in stibnite under ambient conditions. Journal of hazardous materials 385, 121561.

Luo, J., Zhang, H., Santner, J., Davison, W., 2010. Performance characteristics of diffusive gradients in thin films equipped with a binding gel layer containing precipitated ferrihydrite for measuring arsenic (V), selenium (VI), vanadium (V), and antimony (V). Analytical Chemistry 82 (21), 8903–8909.

Macgregor, K., MacKinnon, G., Farmer, J.G., Graham, M.C., 2015. Mobility of antimony, arsenic and lead at a former antimony mine, Glendinning, Scotland. Science of the Total Environment 529, 213–222.

Majzlan, J., Stevko, M., Lánczos, T., 2016. Soluble secondary minerals of antimony in Pezinok and Kremnica (Slovakia) and the question of mobility or immobility of antimony in mine waters. Environmental Chemistry 13 (6), 927–935.

Maresca, V., Heydari, M. and Basile, A., 2020. Antimony and Plants: Accumulation, Toxic Effects, and Plants' Defense Systems. Metalloids in Plants: Advances and Future Prospects, pp.275-299.

Mariussen, E., Johnsen, I.V., Stromseng, A.E., 2017. Distribution and mobility of lead (Pb), copper (Cu), zinc (Zn), and antimony (Sb) from ammunition residues on shooting ranges for small arms located on mires. Environmental Science and Pollution Research 24 (11), 10182–10196.

Mbadugha, L., Cowper, D., Dossanov, S., Paton, G.I., 2020. Geogenic and anthropogenic interactions at a former Sb mine: environmental impacts of As and Sb. Environmental Geochemistry and Health 1–14.

Mensah, A.K., Marschner, B., Antoniadis, V., Stemn, E., Shaheen, S.M., Rinklebe, J., 2021. Human health risk via soil ingestion of potentially toxic elements and remediation potential of native plants near an abandoned mine spoil in Ghana. Science of The Total Environment 798, 149272.

Mishra, S., Dwivedi, J., Kumar, A., Sankararamakrishnan, N., 2016. Removal of antimonite (Sb (III)) and antimonate (Sb (V)) using zerovalent iron decorated functionalized carbon nanotubes. RSC advances 6 (98), 95865–95878.

Mohammadpour, G.A., Karbassi, A.R., Baghvand, A., 2016. Origin and spatial distribution of metals in agricultural soils. Global Journal of Environmental Science and Management 2 (2), 145–156.

Moreno-Andrade, I., Regidor-Alfageme, E., Durazo, A., Field, J.A., Umlauf, K., Sierra-Alvarez, R., 2020. LC-ICP-OES method for antimony speciation analysis in liquid samples. Journal of Environmental Science and Health, Part A 55 (4), 457–463.

Müller, K., Daus, B., Mattusch, J., Vetterlein, D., Merbach, I., Wennrich, R., 2013. Impact of arsenic on uptake and bio-accumulation of antimony by arsenic hyperaccumulator Pteris vittata. Environmental pollution 174, 128–133.

Multani, R.S., Feldmann, T., Demopoulos, G.P., 2016. Antimony in the metallurgical industry: A review of its chemistry and environmental stabilization options. Hydrometallurgy 164, 141–153.

Murciego, A.M., Sánchez, A.G., González, M.R., Gil, E.P., Gordillo, C.T., Fernández, J.C., Triguero, T.B., 2007. Antimony distribution and mobility in topsoils and plants (Cytisus striatus, Cistus ladanifer and Dittrichia viscosa) from polluted Sb-mining areas in Extremadura (Spain). Environmental Pollution 145 (1), 15–21.

Nakamaru, Y.M., Peinado, F.J.M., 2017. Effect of soil organic matter on antimony bioavailability after the remediation process. Environmental Pollution 228, 425–432.

Nam, I.H., Moonk, K.J., Han, Y.S. and Kim, H., 2018, April. Fate and Transport of Antimony on the Sb-resistant Bacterial Growth Isolated from Contaminated Soil. In EGU General Assembly Conference Abstracts (p. 3230). https://ui.adsabs.harvard.edu/abs/2018EGUGA..20.3230N/abstract.

Natasha, Shahid, M., Khalid, S., Dumat, C., Pierart, A., Niazi, N.K., 2019. Biogeochemistry of antimony in soil-plant system: Ecotoxicology and human health. Applied Geochemistry, 106, 45–59.

Ngo, L.K., Pinch, B.M., Bennett, W.W., Teasdale, P.R., Jolley, D.F., 2016. Assessing the uptake of arsenic and antimony from contaminated soil by radish (Raphanus sativus) using DGT and selective extractions. Environmental pollution 216, 104–114.

Nguyen, V.K., Lee, J.U., 2014. Isolation and characterization of antimony-reducing bacteria from sediments collected in the vicinity of an antimony factory. Geomicrobiology Journal 31 (10), 855–861.

NHMRC and NRMMC, 2011. Australian Drinking Water Guidelines Paper 6 National Water Quality Management Strategy. National Health and Medical Research Council, National Resource Management Ministerial Council, Commonwealth of Australia, Canberra.

Ning, Z., Xiao, T., Xiao, E., 2015. Antimony in the soil-plant system in an Sb mining/smelting area of southwest China. International journal of phytoremediation 17 (11), 1081–1089.

Nishad, P.A. and Bhaskarapillai, A., 2021. Antimony, a pollutant of emerging concern: A review on industrial sources and remediation technologies. Chemosphere, p.130252.

NTP, 2018. Report on Carcinogens Monograph on Antimony Trioxide October, Office of the Report on Carcinogens, National Toxicology Program, National Institute of Environmental Health Sciences. National Institutes of Health, Research Triangle Park, US.

Okkenhaug, G., Amstätter, K., LassenBue, H., Cornelissen, G., Breedveld, G.D., Henriksen, T., Mulder, J., 2013. Antimony (Sb) contaminated shooting range soil: Sb mobility and immobilization by soil amendments. Environmental science & technology 47 (12), 6431–6439.

Okkenhaug, G., Gebhardt, K.A.G., Amstaetter, K., Bue, H.L., Herzel, H., Mariussen, E., Almås, Å.R., Cornelissen, G., Breedveld, G.D., Rasmussen, G., Mulder, J., 2016. Antimony (Sb) and lead (Pb) in contaminated shooting range soils: Sb and Pb mobility and immobilization by iron based sorbents, a field study. Journal of hazardous materials 307, 336–343.

Okkenhaug, G., Zhu, Y.G., Luo, L., Lei, M., Li, X., Mulder, J., 2011. Distribution, speciation and availability of antimony (Sb) in soils and terrestrial plants from an active Sb mining area. Environmental Pollution 159 (10), 2427–2434.

Palansooriya, K.N., Shaheen, S.M., Chen, S.S., Tsang, D.C., Hashimoto, Y., Hou, D., Bolan, N.S., Rinklebe, J., Ok, Y.S., 2020. Soil amendments for immobilization of potentially toxic elements in contaminated soils: a critical review. Environment international 134, 105046.

Park, Y., Lee, T., 2019. Microbial antimonate reduction with a solid-state electrode as the sole electron donor: A novel approach for antimony bioremediation. Journal of hazardous materials 377, 179–185.

Pascaud, G., Leveque, T., Soubrand, M., Boussen, S., Joussein, E., Dumat, C., 2014. Environmental and health risk assessment of Pb, Zn, As and Sb in soccer field soils and sediments from mine tailings: solid speciation and bioaccessibility. Environmental Science and Pollution Research 21 (6), 4254–4264.

Pérez-Sirvent, C., Martínez-Sánchez, M.J., Martínez-López, S., Hernández-Córdoba, M., 2011. Antimony distribution in soils and plants near an abandoned mining site. Microchemical Journal 97 (1), 52–56.

Pérez-Sirvent, C., Martínez-Sánchez, M.J., Martínez-López, S., Bech, J., Bolan, N., 2012. Distribution and bioaccumulation of arsenic and antimony in Dittrichia viscosa growing in mining-affected semiarid soils in southeast Spain. Journal of Geochemical Exploration 123, 128–135.

Pierart, A., Shahid, M., Séjalon-Delmas, N., Dumat, C., 2015. Antimony bioavailability: knowledge and research perspectives for sustainable agricultures. Journal of hazardous materials 289, 219–234.

Polack, R., Chen, Y.W., Belzile, N., 2009. Behaviour of Sb (V) in the presence of dissolved sulfide under controlled anoxic aqueous conditions. Chemical Geology 262 (3–4), 179–185.

Prabha, J., Kumar, M., Tripathi, R., 2021. Opportunities and challenges of utilizing energy crops in phytoremediation of environmental pollutants: A review. Bioremediation for Environmental Sustainability 383–396. https://doi.org/10.1016/B978-0-12-820318-7.00017-4.

Protano, G., Nannoni, F., 2018. Influence of ore processing activity on Hg, As and Sb contamination and fractionation in soils in a former mining site of Monte Amiata ore district (Italy). Chemosphere 199, 320–330.

Qi, C., Liu, G., Chou, C.L., Zheng, L., 2008. Environmental geochemistry of antimony in Chinese coals. Science of the Total Environment 389 (2–3), 225–234.

Qi, C., Wu, F., Deng, Q., Liu, G., Mo, C., Liu, B., Zhu, J., 2011. Distribution and accumulation of antimony in plants in the super-large Sb deposit areas. China. Microchemical Journal 97 (1), 44–51.

Ranđelović, D., Mutić, J., Marjanović, P., Đorđević, T., Kašanin-Grubin, M., 2020. Geochemical distribution of selected elements in flotation tailings and soils/sediments from the dam spill at the abandoned antimony mine Stolice. Serbia. Environmental Science and Pollution Research 27 (6), 6253–6268.

Red River Resources Ltd, 2020. (Accessed, April 2021). https://www.asx.com.au/asxpdf/20200929/pdf/44n357g2j7vz2z.pdf.

Reimann, C., Bjorvatn, K., Frengstad, B., Melaku, Z., Tekle-Haimanot, R., Siewers, U., 2003. Drinking water quality in the Ethiopian section of the East African Rift Valley I—data and health aspects. Science of the Total Environment 311 (1–3), 65–80.

Ren, J.H., Ma, L.Q., Sun, H.J., Cai, F., Luo, J., 2014. Antimony uptake, translocation and speciation in rice plants exposed to antimonite and antimonate. Science of the total environment 475, 83–89.

Resongles, E., Casiot, C., Elbaz-Poulichet, F., Freydier, R., Bruneel, O., Piot, C., Delpoux, S., Volant, A., Desoeuvre, A., 2013. Fate of Sb (V) and Sb (III) species along a gradient of pH and oxygen concentration in the Carnoulès mine waters (Southern France). Environmental Science: Processes & Impacts 15 (8), 1536–1544.

Richardson, B.A., 1994. Sudden infant death syndrome: a possible primary cause. Journal-Forensic Science Society 34 (3), 199–204.

Rinklebe, J., Shaheen, S.M., El-Naggar, A., Wang, H., Du Laing, G., Alessi, D.S., Ok, Y.S., 2020. Redox-induced mobilization of Ag, Sb, Sn, and Tl in the dissolved, colloidal and solid phase of a biochar-treated and un-treated mining soil. Environment international 140, 105754.

Rinklebe, J., Shaheen, S.M., Yu, K., 2016. Release of As, Ba, Cd, Cu, Pb, and Sr under predefinite redox conditions in different rice paddy soils originating from the U.S.A. and Asia. Geoderma 270, 21–32.

Saerens, A., Ghosh, M., Verdonck, J., Godderis, L., 2019. Risk of cancer for workers exposed to antimony compounds: a systematic review. Int. J. Environ. Res. Publ. Health 16 (22), 4474.

Sánchez, V., López-Bellido, F.J., Cañizares, P., Villaseñor, J., Rodríguez, L., 2020. Scaling up the electrokinetic-assisted phytoremediation of atrazine-polluted soils using reversal of electrode polarity: A mesocosm study. Journal of environmental management 255, 109806.

Sanderson, P., Naidu, R., Bolan, N., 2014. Ecotoxicity of chemically stabilised metal (loid) s in shooting range soils. Ecotoxicology and environmental safety 100, 201–208.

Sanderson, P., Naidu, R., Bolan, N., Bowman, M., Mclure, S., 2012. Effect of soil type on distribution and bioaccessibility of metal contaminants in shooting range soils. Science of the total environment 438, 452–462.

Schibille, N., Sterrett-Krause, A., Freestone, I.C., 2017. Glass groups, glass supply and recycling in late Roman Carthage. Archaeol Anthropol Sci. 9, 1223–1241.

Schildroth, S., Osborne, G., Smith, A.R., Yip, C., Collins, C., Smith, M.T., Sandy, M.S., Zhang, L., 2020. Occupational exposure to antimony trioxide: a risk assessment. Occup. Environ. Med. https://doi.org/10.1136/oemed-2020-106980 oemed- 2020-106980.

Shaheen, S.M., Abdelrazek, M.A., Elthoth, M., Moghanm, F.S., Mohamed, R., Hamza, A., El-Habashi, N., Wang, J., Rinklebe, J., 2019. Potentially toxic elements in saltmarsh sediments and common reed (Phragmites australis) of Burullus coastal lagoon at North Nile Delta, Egypt: A survey and risk assessment. Science of The Total Environment 649, 1237–1249.

Shaheen, S.M., Rinklebe, J., Frohne, T., White, J.R., DeLaune, R.D., 2014. Biogeochemical factors governing cobalt, nickel, selenium, and vanadium dynamics in periodically flooded Egyptian North Nile Delta rice soils. Soil Science Society of America Journal. 78, 1065–1078.

Shahid, M., Khalid, S., Dumat, C., Pierart, A., Niazi, N.K., 2019. Biogeochemistry of antimony in soil-plant system: Ecotoxicology and human health. Applied Geochemistry 106, 45–59.

Shakerian, F., Dadfarnia, S., Shabani, A.M.H., 2014. Synthesis and characterisation of nano-pore antimony imprinted polymer and its use in the extraction and determination of antimony in water and fruit juice samples. Food Chemistry 145, 571–577.

Shan, J., Ding, X., He, M., Ouyang, W., Lin, C., Liu, X., 2020. Mechanism of birnessite-promoted oxidative dissolution of antimony trioxide. Environmental Chemistry 17 (4), 345–352.

Sharifi, R., Moore, F., Keshavarzi, B., 2016. Mobility and chemical fate of arsenic and antimony in water and sediments of Sarouq River catchment, Takab geothermal field, northwest Iran. Journal of environmental management 170, 136–144.

Silvani, L., Cornelissen, G., Smebye, A.B., Zhang, Y., Okkenhaug, G., Zimmerman, A.R., Thune, G., Sævarsson, H., Hale, S.E., 2019. Can biochar and designer biochar be used to remediate per-and polyfluorinated alkyl substances (PFAS) and lead and antimony contaminated soils? Science of the Total Environment 694, 133693.

Sorvari, J., 2007. Environmental risks at Finnish shooting ranges—a case study. Human and Ecological Risk Assessment: An International Journal 13 (5), 1111–1146.

Sridharan, S., Kumar, M., Bolan, N.S., Singh, L., Kumar, S., Kumar, R., You, S., 2021a. Are microplastics destabilizing the global network of terrestrial and aquatic ecosystem services? Environmental Research, 111243.

Sridharan, S., Kumar, M., Singh, L., Bolan, N.S., Saha, M., 2021b. Microplastics as an emerging source of particulate air pollution: A critical review. Journal of Hazardous Materials, 126245.

Statista, 2021. https://www.statista.com/statistics/264958/antimony-production/. (Accessed, April 2021).

Stromseng, A.E., Ljønes, M., Bakka, L., Mariussen, E., 2009. Episodic discharge of lead, copper and antimony from a Norwegian small arm shooting range. Journal of Environmental Monitoring 11 (6), 1259–1267.

Sun, W., Xiao, E., Xiao, T., Krumins, V., Wang, Q., Häggblom, M., Dong, Y., Tang, S., Hu, M., Li, B., Xia, B., 2017. Response of soil microbial communities to elevated antimony and arsenic contamination indicates the relationship between the innate microbiota and contaminant fractions. Environmental science & technology 51 (16), 9165–9175.

Sun, Y., Kumar, M., Wang, L., Gupta, J., Tsang, D.C., 2020. Biotechnology for soil decontamination: opportunity, challenges, and prospects for pesticide biodegradation. In: Bio-based materials and biotechnologies for eco-efficient construction. Woodhead Publishing, pp. 261–283. https://doi.org/10.1016/B978-0-12-819481-2.00013-1.

Takaoka, M., Fukutani, S., Yamamoto, T., Horiuchi, M., Satta, N., Takeda, N., Oshita, K., Yoneda, M., Morisawa, S., Tanaka, T., 2005. Determination of chemical form of antimony in contaminated soil around a smelter using X-ray absorption fine structure. Analytical Sciences 21 (7), 769–773.

Tan, D., Long, J., Li, B., Ding, D., Du, H., Lei, M., 2018. Fraction and mobility of antimony and arsenic in three polluted soils: a comparison of single extraction and sequential extraction. Chemosphere 213, 533–540.

Tandy, S., Meier, N., Schulin, R., 2017. Use of soil amendments to immobilize antimony and lead in moderately contaminated shooting range soils. Journal of hazardous materials 324, 617–625.

Tella, M., Pokrovski, G.S., 2009. Antimony (III) complexing with O-bearing organic ligands in aqueous solution: An X-ray absorption fine structure spectroscopy and solubility study. Geochimica et Cosmochimica Acta 73 (2), 268–290.

Thestorf, K., Makki, M., 2021. Pseudo-total antimony content in topsoils of the Berlin Metropolitan Area. Journal of Soils and Sediments 21 (5), 2102–2117.

Tian, H., Zhou, J., Zhu, C., Zhao, D., Gao, J., Hao, J., He, M., Liu, K., Wang, K., Hua, S., 2014. A comprehensive global inventory of atmospheric antimony emissions from anthropogenic activities, 1995–2010. Environmental science & technology 48 (17), 10235–10241.

Tian, H.Z., Zhao, D., He, M.C., Wang, Y., Cheng, K., 2011. Temporal and spatial distribution of atmospheric antimony emission inventories from coal combustion in China. Environmental Pollution 159 (6), 1613–1619.

Tighe, M., Ashley, P., Lockwood, P., Wilson, S., 2005. Soil, water, and pasture enrichment of antimony and arsenic within a coastal floodplain system. Science of the Total Environment 347 (1–3), 175–186.

Tschan, M., Robinson, B., Johnson, C.A., Bürgi, A., Schulin, R., 2010. Antimony uptake and toxicity in sunflower and maize growing in Sb III and Sb V contaminated soil. Plant and soil 334 (1), 235–245.

Tschan, M., Robinson, B.H., Schulin, R., 2009. Antimony in the soil–plant system-a review. Environmental chemistry 6 (2), 106–115.

Tserenpil, S., Liu, C.Q., 2011. Study of antimony (III) binding to soil humic acid from an antimony smelting site. Microchemical journal 98 (1), 15–20.

Turner, A., Filella, M., 2017. Field-portable-XRF reveals the ubiquity of antimony in plastic consumer products. Science of the total Environment 584, 982–989.

Turner, A., 2018. Black plastics: Linear and circular economies, hazardous additives and marine pollution. Environment international 117, 308–318.

United States Geological Survey (USGS), 2021. https://pubs.usgs.gov/periodicals/mcs2021/mcs2021-antimony.pdf. (Accessed, August 2021).

US-PHS 1992. Toxicological profile of antimony and compounds Agency for Toxic Substances and Disease Registry U.S. Public Health Service.

Vikent'eva, O. and Vikentev, I., 2016, April. Occurrence modes of As, Sb, Te, Bi, Ag in sulfide assemblages of gold deposits of the Urals. In IOP Conference Series: Materials Science and Engineering (Vol. 123, No. 1, p. 012028). IOP Publishing.

Wan, X.M., Tandy, S., Hockmann, K., Schulin, R., 2013. Changes in Sb speciation with waterlogging of shooting range soils and impacts on plant uptake. Environmental Pollution 172, 53–60.

Wang, H., Lv, Z., Song, Y., Wang, Y.N., Zhang, D., Sun, Y., Tsang, Y.F., Pan, X., 2019a. Adsorptive removal of Sb (III) from wastewater by environmentally-friendly biogenic manganese oxide (BMO) materials: Efficiency and mechanisms. Process Safety and Environmental Protection 124, 223–230.

Wang, H., Lv, Z., Wang, B., Wang, Y.N., Sun, Y., Tsang, Y.F., Zhao, J., Zhan, M., 2019b. Effective stabilization of antimony in Waste-to-Energy fly ash with recycled laboratory iron–rich residuals. Journal of Cleaner Production 230, 685–693.

Wang, N., Wang, A., Kong, L., He, M., 2018. Calculation and application of Sb toxicity coefficient for potential ecological risk assessment. Science of the Total Environment 610, 167–174.

Wang, X., He, M., Xi, J., Lu, X., 2011. Antimony distribution and mobility in rivers around the world's largest antimony mine of Xikuangshan, Hunan Province China. Microchemical Journal 97 (1), 4–11.

Wang, Y.Y., Ji, H.Y., Lyu, H.H., Liu, Y.X., He, L.L., You, L.C., Zhou, C.H., Yang, S.M., 2019c. Simultaneous alleviation of Sb and Cd availability in contaminated soil and accumulation in Lolium multiflorum Lam. After amendment with Fe–Mn-Modified biochar. Journal of cleaner production 231, 556–564.

Warnken, J., Ohlsson, R., Welsh, D.T., Teasdale, P.R., Chelsky, A., Bennett, W.W., 2017. Antimony and arsenic exhibit contrasting spatial distributions in the sediment and vegetation of a contaminated wetland. Chemosphere 180, 388–395.

Wei, C., Ge, Z., Chu, W., Feng, R., 2015. Speciation of antimony and arsenic in the soils and plants in an old antimony mine. Environmental and experimental botany 109, 31–39.

Wei, Y., Su, Q., Sun, Z., Shen, Y., Li, J., Zhu, X., Hou, H., Chen, Z., Wu, F.C., 2016. The role of arbuscular mycorrhizal fungi in plant uptake, fractions, and speciation of antimony. Applied Soil Ecology 107, 244–250.

Wersin, P., Johnson, C.A., Furrer, G., 2002. August. Antimony contamination in soil and ground water by shooting range activities. In Geochimica et Cosmochimica Acta 66 (No. 15 A).

WHO, 2011. Fourth Edition. Guidelines for drinking-water quality. WHO Chronicle 38 (4), 104–108.

Wilson, S.C., Leech, C.D., Butler, L., Lisle, L., Ashley, P.M., Lockwood, P.V., 2013. Effects of nutrient and lime additions in mine site rehabilitation strategies on the accumulation of antimony and arsenic by native Australian plants. Journal of hazardous materials 261, 801–807.

Wilson, S.C., Lockwood, P.V., Ashley, P.M., Tighe, M., 2010. The chemistry and behaviour of antimony in the soil environment with comparisons to arsenic: a critical review. Environmental pollution 158 (5), 1169–1181.

Wilson, S.C., Tighe, M., Paterson, E., Ashley, P.M., 2014. Food crop accumulation and bioavailability assessment for antimony (Sb) compared with arsenic (As) in contaminated soils. Environmental Science and Pollution Research 21 (20), 11671–11681.

Wu, F., Fu, Z., Liu, B., Mo, C., Chen, B., Corns, W., Liao, H., 2011a. Health risk associated with dietary co-exposure to high levels of antimony and arsenic in the world's largest antimony mine area. Science of the Total Environment 409 (18), 3344–3351.

Wu, X.D., Song, J.M., Li, X.G., Yuan, H.M., Li, N., 2011b. Behaviors of dissolved antimony in the Yangtze River Estuary and its adjacent waters. Journal of Environmental Monitoring 13 (8), 2292–2303.

Wuana, R.A. and Okieimen, F.E., 2011. Heavy metals in contaminated soils: a review of sources, chemistry, risks and best available strategies for remediation. International Scholarly Research Notices, 2011.

Wysocki, R., Chéry, C.C., Wawrzycka, D., Van Hulle, M., Cornelis, R., Thevelein, J.M., Tamás, M.J., 2001. The glycerol channel Fps1p mediates the uptake of arsenite and antimonite in Saccharomyces cerevisiae. Molecular microbiology 40 (6), 1391–1401.

Xu, W., Wang, H., Liu, R., Zhao, X., Qu, J., 2011. The mechanism of antimony (III) removal and its reactions on the surfaces of Fe–Mn binary oxide. Journal of colloid and interface science 363 (1), 320–326.

Xu, Y.H., Ohki, A., Maeda, S., 2001. Adsorption and removal of antimony from aqueous solution by an activated alumina: 1. Adsorption capacity of adsorbent and effect of process variables. Toxicological & Environmental Chemistry 80 (3–4), 133–144.

Xue, S., Shi, L., Wu, C., Wu, H., Qin, Y., Pan, W., Hartley, W., Cui, M., 2017. Cadmium, lead, and arsenic contamination in paddy soils of a mining area and their exposure effects on human HEPG2 and keratinocyte cell-lines. Environmental research 156, 23–30.

Yan, G., Mao, L., Jiang, B., Chen, X., Gao, Y., Chen, C., Li, F., Chen, L., 2020. The source apportionment, pollution characteristic and mobility of Sb in roadside soils affected by traffic and industrial activities. Journal of Hazardous Materials 384, 121352.

Yang, X., Shi, Z., Liu, L., 2015. Adsorption of Sb (III) from aqueous solution by QFGO particles in batch and fixed-bed systems. Chemical Engineering Journal 260, 444–453.

Yu, T.C., Wang, X.H., Li, C., 2014. Removal of antimony by FeCl 3-modified granular-activated carbon in aqueous solution. Journal of Environmental Engineering 140 (9), A4014001.

Zand, A.D., Heir, A.V., 2020. Phytoremediation: Data on effects of titanium dioxide nanoparticles on phytoremediation of antimony polluted soil. Data in Brief 31, 105959.

Zeng, D., Zhou, S., Ren, B. and Chen, T., 2015. Bioaccumulation of antimony and arsenic in vegetables and health risk assessment in the superlarge antimony-mining area, China. Journal of analytical methods in chemistry, 2015.

Zhang, J., Deng, R., Ren, B., Yaseen, M., Hursthouse, A., 2020. Enhancing the removal of Sb (III) from water: A Fe3O4@ HCO composite adsorbent caged in sodium alginate microbeads. Processes 8 (1), 44.

Zhang, M., Kolton, M., Li, Z., Lin, H., Li, F., Lu, G., Gao, P., Sun, X., Xu, R., Xu, F., Sun, W., 2021a. Bacteria responsible for antimonite oxidation in antimony-contaminated soil revealed by DNA-SIP coupled to metagenomics. FEMS Microbiology Ecology 97 (5), p.fiab057.

Zhang, S., Wang, Y., Pervaiz, A., Kong, L., He, M., 2018. Comparison of diffusive gradients in thin-films (DGT) and chemical extraction methods for predicting bioavailability of antimony and arsenic to maize. Geoderma 332, 1–9.

Zhang, X., Liu, T., Li, F., Li, X., Du, Y., Yu, H., Wang, X., Liu, C., Feng, M., Liao, B., 2021b. Multiple effects of nitrate amendment on the transport, transformation and bioavailability of antimony in a paddy soil-rice plant system. Journal of Environmental Sciences 100, 90–98.

Zhong, Q., Ma, C., Chu, J., Wang, X., Liu, X., Ouyang, W., Lin, C., He, M., 2020. Toxicity and bioavailability of antimony in edible amaranth (Amaranthus tricolor Linn.) cultivated in two agricultural soil types. Environmental Pollution 257, 113642.

Zhou, S., Deng, R., Hursthouse, A., 2020. Risk assessment of potentially toxic elements pollution from mineral processing steps at Xikuangshan antimony plant, Hunan, China. Processes 8 (1), 29.

Zhou, S., Hursthouse, A. and Chen, T., 2019. Pollution characteristics of Sb, As, Hg, Pb, Cd, and Zn in soils from different zones of Xikuangshan antimony mine. Journal of analytical methods in chemistry, 2019.

Zhou, X., Sun, C., Zhu, P., Liu, F., 2018. Effects of antimony stress on photosynthesis and growth of Acorus calamus. Frontiers in plant science 9, 579.

Zhu, Y., Yang, J., Wang, L., Lin, Z., Dai, J., Wang, R., Yu, Y., Liu, H., Rensing, C. and Feng, R., 2020. Factors influencing the uptake and speciation transformation of antimony in the soil-plant system, and the redistribution and toxicity of antimony in plants. Science of The Total Environment, p.140232.

Zhuang, W., Lai, X., Wang, Q., Liu, Y., Chen, Q., Liu, C., 2018. Distribution characteristics, sources and ecological risk of antimony in the surface sediments of Changjiang Estuary and the adjacent sea, East China. Marine pollution bulletin 137, 474–480.